Choosing the Right Fluorescent Probe

Maria J. Sarmento and Fábio Fernandes

Contents

Abstract Fluorescence microscopy and spectroscopy are by now used routinely in any laboratory working on the field of basic and applied biological sciences. A wide and expanding library of small organic fluorophores with radically different properties has been made available, offering great flexibility to the user of fluorescence-based methods. Beyond small organic fluorophores, the development of fluorescent proteins allowed for the introduction of genetically encoded fluorescence tagging, a novel tool that quickly revolutionized cellular imaging and cell biology.

M. J. Sarmento (✉)
Instituto de Medicina Molecular, Faculdade de Medicina, Universidade de Lisboa, Lisbon, Portugal
e-mail: maria.sarmento@medicina.ulisboa.pt

F. Fernandes
iBB – Institute for Bioengineering and Biosciences, Instituto Superior Técnico, Universidade de Lisboa, Lisbon, Portugal

Associate Laboratory i4HB – Institute for Health and Bioeconomy, IST, Universidade de Lisboa, Lisbon, Portugal

Department of Bioengineering, Instituto Superior Técnico, Universidade de Lisboa, Lisbon, Portugal
e-mail: fernandesf@tecnico.ulisboa.pt

R. Šachl, M. Amaro (eds.), *Fluorescence Spectroscopy and Microscopy in Biology*, Springer Ser Fluoresc (2023) 20: 3–52, https://doi.org/10.1007/4243_2022_30, Published online: 3 January 2023

Still, a considerable fraction of casual users of fluorescence tools do not follow rational considerations when selecting a fluorescent probe for their intended application, often relying on trial and error alone, which inevitably leads to a decrease in data quality and limits the potential of fluorescence-based methods. This chapter aims to present an overview of the most important considerations to be made when selecting a fluorescent reporter. Fluorophore properties and their importance for fluorescence assays will be discussed. A list of different fluorophores and a summary of their properties will also be presented as a tool to assist in the process of choosing the right fluorescence probe. Finally, specific applications such as super-resolution microscopy require very specific fluorophores, and these will be discussed separately.

Keywords Fluorescence · Fluorescent proteins · Labelling · Organic probes · Super-resolution microscopy

The popularity of fluorescence methods in biology is largely associated with their extraordinary sensitivity and flexibility. Nevertheless, the quality of fluorescence-based assays is still fundamentally limited by factors such as number of detected photons, so that the choice of adequate fluorescent probe is pivotal in dictating the quality of fluorescence data.

Organic fluorescent compounds typically present aromatic or conjugated double bonds. Lipids and nucleic acids do not generally present fluorescence, while proteins commonly exhibit fluorescence in the UV range, and in some cases also in the visible range of the spectra [1]. Intrinsic fluorophores are the ones that occur naturally, while extrinsic fluorophores are added to a sample.

1 Intrinsic and Extrinsic Fluorescent Probes

Intrinsic fluorescence or autofluorescence results from the presence of molecules that are naturally fluorescent [2, 3], such as NADH, flavins and porphyrins. These molecules have been used at times as indicators of particular cellular processes [4, 5], but their sparse abundance and poor photophysical properties strictly limit their application. Autofluorescence can also arise from the presence of the aromatic amino acids tryptophan (Trp), tyrosine (Tyr) and phenylalanine (Phe). Particularly, Trp has been extensively used in seminal works on protein conformation and interactions due to its ability to report on the local microenvironment, either through variation in fluorescence intensity and/or the spectral shift of the emission peak [6–9]. However, the study of a particular protein within the cellular environment is impossible, as a multitude of different proteins present one or more tryptophan residues. Bulk Trp fluorescence has still been proven useful to distinguish, for example, oesophageal cancer cells from their healthy counterparts [10], and to monitor bacteria inactivation upon UV light exposure [11]. It is important to mention

that molecules such as collagen and elastin also present intrinsic fluorescence, and so the extracellular matrix can also contribute to the overall autofluorescence of the samples [3].

To circumvent these issues, over the past decades extrinsic fluorescence has been extensively explored through the development of a wide variety of fluorophores with improved photophysical properties and capable of very high molecular selectivity [12]. These fluorophores comprise three main classes: organic dyes [13–15], fluorescent proteins [16, 17] and inorganic probes. The latter group, however, that includes quantum dots [18–23], metal complexes [24–26], lanthanide complexes/nanoparticles [27–30] and carbon dots/nanoparticles [31–34], still presents some strong drawbacks that prevent their extensive application in living cells when compared to the other two. Quantum dots, for example, can exhibit significant toxicity mainly due to their heavy metal core and the formation of free radicals upon excitation [35]. Moreover, the need for specific coating to assure selectivity renders quantum dots potentially even larger than a fluorescent protein, hindering their ability to enter the cells through diffusion [35, 36]. Their internalization is then dependent on the physiological internalization processes of the cell or the coupling with molecules able to facilitate the cellular uptake. In this review, we will thus focus on organic probes and fluorescent proteins (FPs), but thorough revisions of the properties and applications of inorganic dyes can be found elsewhere [37].

In general, any extrinsic probe used for live-cell imaging should fulfil defined pre-requisites, also depending on the particular application/technique. Targeting of the molecule or structure of interest must be as specific as possible. Lack of selectivity, even in a small extent, can lead to misinterpretation of the data, even more so in highly sensitive techniques such as single-molecule fluorescence and super-resolution microscopy. The detectability of the probe in the cellular context is also crucial. The photon yield of the probe must be sufficient to allow proper detection of the target molecule at its physiological levels. However, this should not be accomplished through the unreasonable increase of the probe's concentration since it will possibly interfere with the studied intracellular process. The dye should also allow for the use of a low excitation power to prevent any cellular photodamage. Furthermore, recent years have witnessed an increased demand for far-red to near-infrared emitting dyes [38–41]. This class of dyes work in a spectral range where biological samples are actually transparent, thus avoiding autofluorescence, besides reducing part of the spectral overcrowding in multi-channel imaging.

2 Organic Dyes

Arguably the most popular small organic fluorophore, fluorescein, a xanthene-based dye (Fig. 1), was synthesized in the nineteenth century by Baeyer [42] and remains ubiquitous for standard applications in fluorescence spectroscopy and microscopy. Since then, a multitude of different fluorophores and derivatives with different properties have been made available to researchers in biological sciences

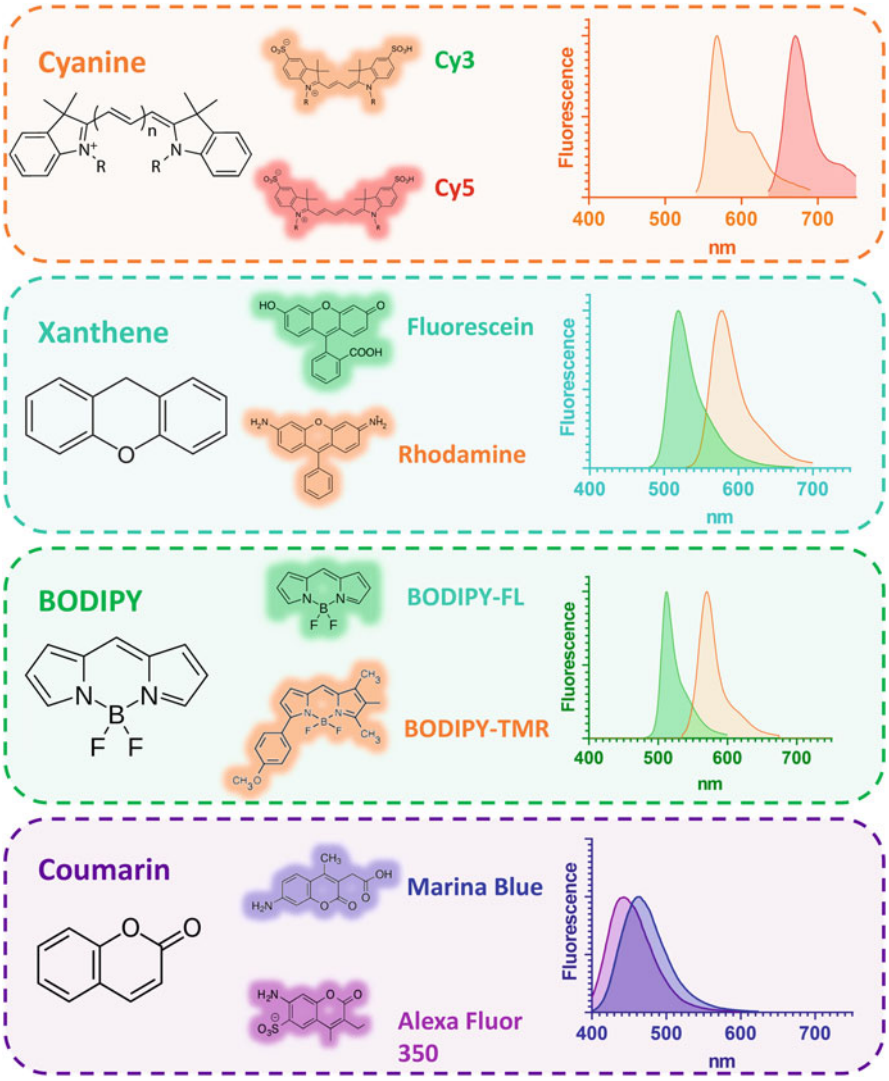

Fig. 1 Popular classes of extrinsic fluorescent probes for life sciences applications. Examples of each class are presented together with the corresponding fluorescence emission spectra

(Table 1). These are by now used in countless applications, from the study of very specific biological processes, such as protein folding and cellular distribution, macromolecule interactions, endocytosis and DNA replication, just to name a few, to the development of different sensors, including for virus detection, and the determination of biological microenvironment properties as membrane potential, viscosity and redox potential [1]. This functional versatility is intimately related with

Table 1 Properties and applications of some of the most popular organic probes used in life sciences

Probe	$\lambda_{max,abs}$ (nm)	$\lambda_{max,em}$ (nm)	τ (ns)	Applications and notes	References
Alexa Fluor 350	346	442	–	UV-excitable dye. Small fluorophore Brighter than AMCA	[43]
Alexa Fluor 488	494	517	4.1	Popular bright green fluorophore	[44, 45]
Alexa Fluor 594	590	617	4.0	Significantly brighter than Texas Red	[44, 46]
Alexa Fluor 633	632	647	3.2	Far-red fluorescence	[43, 47]
Alexa Fluor 647	651	672	1	Far-red fluorescence	[47]
AMCA	349	448	4	Commonly used UV-excitable dye Small fluorophore	[43, 48]
ATTO 488	500	525	4.2	Popular bright green fluorophore	[49]
ATTO 647 N	644	669	2.4	Highly photostable. Very hydrophobic and cationic. Used in high-resolution microscopy	[50]
ATTO 655	633	684	1.8–3.7	Far-red fluorescence. Quenched by Trp and Guanosine. Lifetime sensitive to DNA binding	[51, 52]
ATTO 680	680	700	1.7	Far-red fluorescence. Quenched by Trp and Guanosine	[52]
BODIPY 630/650	625	640	3.9	Narrow emission band. Small Stokes shift	[43]
BODIPY 650/665	646	660		Longest-wavelength BODIPY dye. Narrow emission band. Small Stokes shift	[43]
BODIPY FL	505	513	5.7	Narrow emission band. Small Stokes shift Insensitive to pH (unlike fluorescein) Relatively long lifetime	[53]
BODIPY-TMR	542	574	5.1	Narrow emission band, photoresistant	[43, 54]
Cy3	548	562	0.3	Commonly used hydrophobic yellow cyanine. Used for labelling of oligonucleotides and antibodies. Sulfo-Cy3 presents higher water solubility	[47, 55]
Cy3B	558	572	2.8	Rigidized cyanine with higher fluorescence quantum yield and lifetime than Cy3	[47, 55]

(continued)

Table 1 (continued)

Probe	$\lambda_{max,abs}$ (nm)	$\lambda_{max,em}$ (nm)	τ (ns)	Applications and notes	References
Cy5	646	663	0.98	Commonly used hydrophobic far-red cyanine. Used for labelling of oligonucleotides and antibodies. Sulfo-Cy5 presents higher water solubility	[56]
Cy5.5	675	694	1	Near-IR cyanine. Used for labelling of oligonucleotides and antibodies. Sulfo-Cy5.5 presents considerably higher water solubility	[47]
DiD/DiIC$_{18}$(5)	644	665	~1	Lipophilic dialkylcarbocyanine dye for membrane labelling. Allows for long-term cell tracking	[43]
DiI/DiIC$_{18}$(3)	549	564	1–1.5[a]	Lipophilic dialkylcarbocyanine dye for membrane labelling. Allow for long-term cell tracking	[43, 57]
DPH (MeOH)	350	428	5.0[b]	Membrane viscosity probe	[58, 59]
EDANS	336	520	8.9	Protein labelling, environment sensing, long lifetime	[43, 60]
FITC	494	518	3.7	Commonly used fluorescein derivative for covalent labelling of biomolecules Prone to photobleaching	[61]
Fluorescein (dianion, pH above 6.4)	491	515	4.2	Fluorescence spectroscopy and microscopy in general	[62–64]
Hoechst 33342 (ds DNA)	350	456	2.2	Nuclei imaging, flow cytometry, detection of DNA	[47]
Hoechst 33342 (no DNA)	336	471	0.35	Nuclei imaging, flow cytometry, detection of DNA	[47]
Laurdan (in lipid membranes)	~355	440–490	4–5.9	Measurement of lipid membrane hydration and order	[65]
NBD[c]	478	545	1–10	FRAP, protein labelling, environment sensing	[66–68]
Nile Red (EtOH)	554	629	3.65	Lipophilic stain. Useful for labelling intracellular lipid droplets. Almost non-fluorescent in water	[69, 70]
Pyrene (in cyclohexane)	338	375	100–400	Very long lifetime. Forms excimers which allow for detection of conformational changes of macromolecules or subunit assembly	[43]
Rhodamine 110	505	534	4.0	Frequently used in substrates for protease activity assays	[47]
Rhodamine 6G	526	556	3.9	Commonly used cationic dye. Very photostable	[55]

Rhodamine B	557	578	1.43	Commonly used hydrophobic dye	[55]
SR101	578	605	–	Frequently used for selective astrocyte labelling in neurophysiological experiments	[43, 71]
TRITC	554	573	2.2	Commonly used bright orange dye for labelling of biomolecules	[44, 45]
Texas Red	596	620	4.2	Sulfonyl chloride derivative of SR101 used for conjugation of proteins and oligonucleotides	[44, 47]
TMA-DPH (MeOH)	356	451	0.27	Membrane viscosity probe	[72]
YOYO-1(bound to DNA)	490	507	2.3	Useful for detection of nucleic acids (quantum yield of DNA bound molecule is far superior to the one of free dye)	[47]
YOYO-1(no DNA)	457	549	2.1	–	[47]
YOYO-3	612	631	–	Membrane impermeable DNA-binding dye. Useful for monitoring cell viability	[43]

Unless specified, values are shown for the probes in water

AMCA 7-amino-4-methylcoumarin, *DiD/DiI* 1,1′-dioctadecyl-3,3,3′,3′-tetramethylindodicarbocyanine, *DPH* 1,6-diphenyl-1,3,5-hexatriene, *EDANS* 5-(2-aminoethylamino)-1-naphthalenesulfonic acid, *FITC* fluorescein-5-isothiocyanate, *NBD* 4-nitrobenz-2-oxa-1,3-diazole, *SR101* sulforhodamine 101, *TRITC* tetramethylrhodamine, *TMA-DPH* 1-(4-trimethylammoniumphenyl)-6-phenyl-1,3,5-hexatriene p-toluenesulfonate

[a] Lifetime values measured in live cells

[b] Measured in ethanol

[c] Emission properties of NBD are highly sensitive to solvent polarity, and the quantum yield in water approaches 0. Hence the spectral properties depicted are for the fluorophore in DMSO

some unique features that overcome some of the limitations of FPs (as described in Sect. 3) [73]. Possibly the most significant of these features is their much smaller size, limiting the impact of the dye on biological functions and properties of the target molecules [74]. Historically, another main advantage of organic probes over FPs is their superior photophysical properties (e.g. higher photostability), resulting in a higher photon yield [75] and, consequently, higher quality data. However, this gap has been decreasing over the years due to the development of better performing FPs. They also outshine FPs in terms of labelling versatility. First, organic probes offer the possibility of labelling proteins at various positions, not being limited to the terminal residues. Second, labelling is not restricted to proteins, and thus any molecular structure from DNA to lipids can in principle be tagged through bioorthogonal chemistry.

Despite all the advantages, there are still some limitations that preclude the use of these molecules in particular experiments. For example, synthetic dyes are not genetically encoded, and thus the degree of labelling of a particular target might interfere with the acquisition of quantitative data. Furthermore, when it comes to labelling intracellular structures, the probes must have some solubility in aqueous media but should also be cell-permeant. However, membrane permeability depends on properties such as size, lipophilicity and charge [76], and so several probes have to be loaded into the cell through alternative methods (e.g. microinjection) [77]. An additional problem that frequently arises from loading cells with fluorescent synthetic probes is the non-specific adsorption of these molecules to different cell structures, leading to significant background fluorescence. In this case, extensive washing cycles are often required, which in turn may be incompatible with particular applications involving time-tracking of fast biological functions. This limitation however has been overcome through the development of the so-called smart (or fluorogenic) probes [73, 78]. These probes are initially quenched, emitting very weak or no fluorescence. Upon interaction with the target molecule, a chemical or conformational alteration renders the probe fluorescent at specific wavelengths. One of the most popular examples of smart probes are the DNA-binding cyanines TOTO and YOYO. Both probes are non-fluorescent in aqueous solution. Intercalation with DNA forces the molecules into a fluorescent planar form [79, 80].

Four classes of organic fluorophores have become particularly popular as extrinsic fluorescent probes for life sciences applications. These are cyanines, xanthenes, BODIPY and coumarins (Fig. 1). Although a comprehensive description of all available synthetic fluorophores, their applications and experimental considerations is out of the scope of this chapter, we will present valuable information to help users to choose the appropriate organic dye and experimental design that would ultimately fit their needs. Fundamental photophysical properties will be introduced and their relevance for a successful fluorescence-based experiment will be discussed. The properties of selected examples of commercially available organic dyes will also be presented (Sect. 2.1 and Table 1). Then, several labelling strategies are also described (Sect. 2.2). Finally, due to their intrinsically different properties and experimental requirements, a concise description of membrane probes and their main applications is also included (Sect. 2.3).

2.1 Ideal Properties of Fluorescent Probes

In a fluorescence experiment, the fluorophore will cycle between the ground and excited states, and fluorescence is obtained upon radiative return to the ground state (Fig. 2).

Typically, a single fluorophore can undergo several thousand repeats of this cycle before destruction [1], and this is largely responsible for the extraordinary sensitivity of fluorescence methods. Importantly, due to the presence of multiple processes contributing to the dissipation of energy from the excited state (Fig. 2a), the energy of the fluorescence photon is smaller than the energy of excitation. This shift to a longer wavelength is known as the Stokes shift (Fig. 2b) and is critical to the sensitivity of fluorescence-based methods, as blocking of the excitation light allows for selective detection of fluorescence light [81].

The most important properties of the fluorophore dictate the pattern of the cycle between ground and excited states, and we will discuss them individually in the next sections.

2.1.1 Molecular Brightness

The molecular brightness (B) of a fluorophore, defined as the number of photons per second for a single molecule, is not an intrinsic property of the molecule, as it depends on the excitation intensity, as well as on light collection and detection

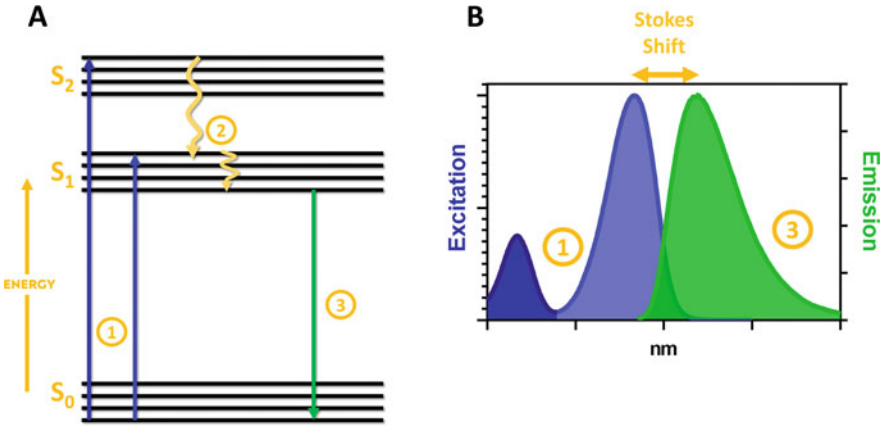

Fig. 2 Excitation and emission of a fluorophore. (**a**) Jablonski diagram depicting the excitation of a fluorophore through absorbance of light (1), creating an excited electronic singlet state (S1 or S2), followed by dissipation of energy through internal conversion, vibrational or solvent relaxation (2). Fluorescence emission takes place upon return to the ground state (3). (**b**) Fluorescence excitation and emission spectra of a fluorophore

efficiency by the instrument during acquisition [1]. Nevertheless, it is proportional to the product of the molar extinction coefficient (ε) at the excitation wavelength and the fluorescence quantum yield (QY) of the molecule [1]:

$$B \approx \varepsilon \times \mathrm{QY} \tag{1}$$

In most applications, the number of photons acquired dictates the quality of recovered data. In many experiments, the impact of a low brightness value can be compensated by increasing the concentration of the fluorophore in the sample or by increasing the excitation intensity. However, when this is not possible, as is often the case for fluorescence microscopy applications, a very high B value is desirable in order to avoid the use of very high-intensity excitation light. The use of high-intensity excitation light can lead to increased background signal, contamination of detection by excitation light and decreased fluorophore stability (see below). The higher the value of B is, the lower the excitation intensity can be to achieve sufficient fluorescence photon counts.

Low brightness of labelled molecules, as defined in Eq. 1, can be certainly compensated by increasing the stoichiometry of dyes to macromolecule (D:M). However, the drawback of such strategy is that the structure or pattern of molecular interactions of the labelled molecule can be negatively impacted. In the case of labelled antibodies, increasing the degree of labelling (DOL, mean number of fluorophores per antibody) leads to sharp decreases in antibody affinity [82, 83]. Additionally, in the case of specific labelling strategies, an increase in D:M stoichiometry could be impossible. For these reasons, the use of probes offering adequately high values of ε and QY is strongly recommended.

2.1.2 Extinction Coefficient

The molar extinction coefficient of a molecule (in M^{-1} cm^{-1}) describes the capacity for light absorption at a given wavelength. The cross-section for light absorption (σ) of a fluorophore describes the photon capture area of a molecule and is calculated from ε using [1]:

$$\sigma = 3.82 \times 10^{-5} \varepsilon \left(\text{in } \text{Å}^2 \right) \tag{2}$$

In the case of fluorescein, which presents a considerable ε value of 75,500 M^{-1} cm^{-1} at 490 nm [62] (Fig. 3), the cross-section value for light absorption is 2.88 $Å^2$, which is significantly smaller than its molecular dimensions. In this way, only a small fraction of light encountered by the fluorophore is effectively absorbed by it.

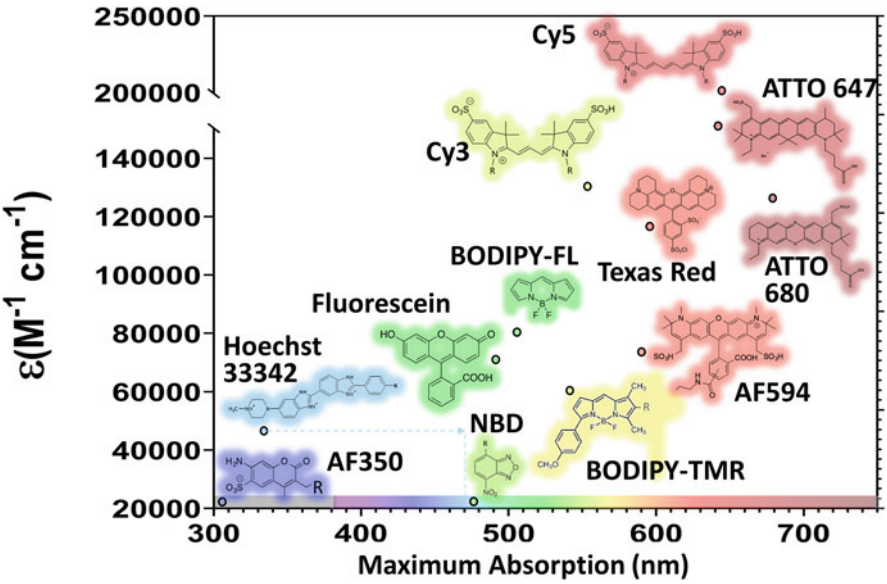

Fig. 3 Extinction coefficients (ε) and absorption maximum (λ_{Abs}^{max}) for a selection of commonly used fluorophores. Exact values of ε and λ_{Abs}^{max} correspond to the positions of open circles closer to each fluorophore. Colours associated with each structure reflect the wavelength of maximum fluorescence emission according to the colour spectrum shown in the bottom. The Stokes shift for Hoechst 33342 (unbound) is represented by an arrow. Cy3 and Cy5 are shown in their sulfonated forms. Values taken from [43, 44, 56, 60, 63, 64, 66, 84–87]

2.1.3 Quantum Yield

Fluorescence quantum yield (QY) is defined as the ratio of the number of photons emitted to the number of photons absorbed. Since the fluorophore molecule can also return to the ground state from the excited state through nonradiative processes, the value of QY is always smaller than 1. Taking once more fluorescein as an example, its quantum yield is 0.93 at 490 nm [62] (Fig. 4). This large QY value is largely responsible for the popularity of fluorescein as a fluorophore. Values of quantum yield are generally listed at the wavelength of maximum absorption.

The presence of efficient electron donors in the vicinity of the fluorophore has been shown to lead to marked decreases in quantum yield. The amino acid tryptophan and to a lesser degree tyrosine, methionine and histidine have been shown to decrease the quantum yield of a large array of fluorophores by different combinations of static and dynamic quenching [88, 89]. On the other hand, carbocyanines, such as Cy3, Cy5 (Fig. 1) or Alexa Fluor 647 (AF647) (Figs. 3 and 4), have been shown to be less susceptible to intramolecular quenching by these amino acids [89]. Similar quenching of fluorophores has been reported for labelled oligonucleotides, as specific nucleotides, namely guanosine, induce significant quenching of several fluorophores in their immediate vicinity [89]. Oxazine derivatives such as

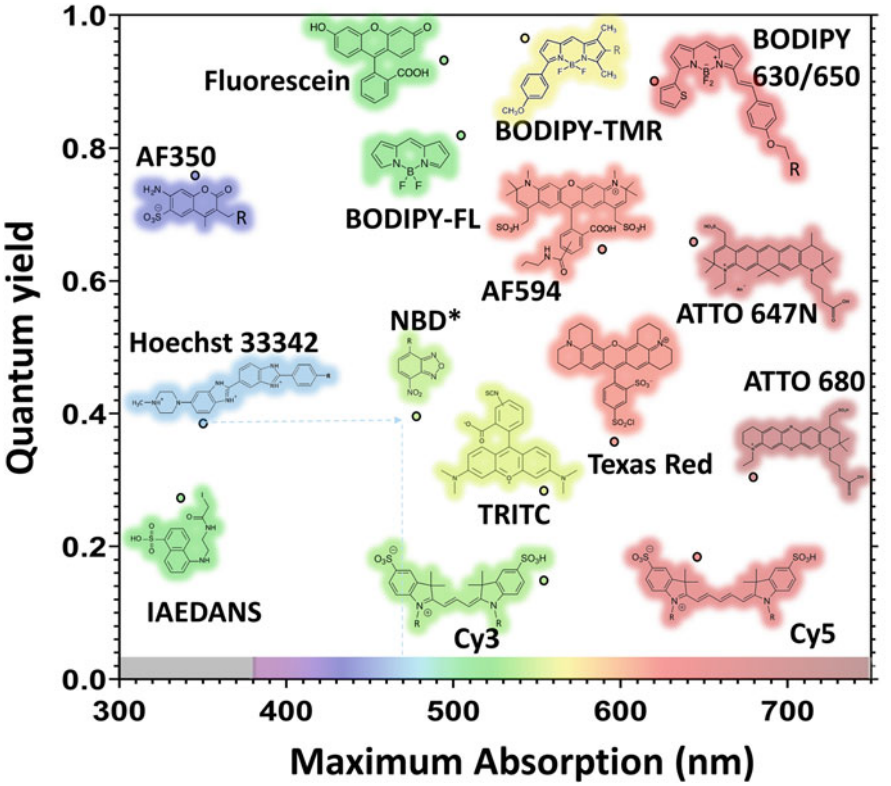

Fig. 4 Fluorescence quantum yield (QY) and absorption maximum (λ_{Abs}^{max}) for a selection of commonly used fluorophores. Exact values of quantum yield and λ_{Abs}^{max} correspond to the positions of open circles closer to each fluorophore. Colours associated with each structure reflect the wavelength of maximum fluorescence emission according to the colour spectrum shown in the bottom. The Stokes shift for Hoechst 33342 (unbound) is represented by an arrow. *Properties of NBD are for the fluorophore in DMSO, as its quantum yield approaches 0 in water. Cy3 and Cy5 are shown in their sulfonated forms. Values taken from [43, 44, 56, 60, 63, 64, 66, 84–87]

ATTO 655 and ATTO 680 (Figs. 2 and 3) are particularly susceptible to these effects, and this has been used to detect peptide–antibody interactions with labelled peptides [90].

2.1.4 Photostability

One of the most important parameters to be considered when choosing a fluorescent probe is its photoresistance, especially when the goal is its use for imaging applications. In fact, one of the most limiting factors in defining fluorescence intensity in fluorescence microscopy is the irreversible photochemical destruction of the

fluorophore during continuous illumination. The rate of this process, called photobleaching, determines the number of photons a fluorophore can emit before its destruction [1]. In practice, photobleaching results in a decrease in fluorescence emission overtime during acquisition, as larger fractions of fluorophores are photodamaged.

The average number of photons a fluorophore can emit before its destruction can be estimated based on its quantum yield and photobleaching rates [1]. Fluorophores usually used in fluorescence microscopy applications emit from 10^4 to 10^6 photons during their useful lifetime, while other molecules can only emit around 1,000 photons before irreversible destruction [1, 91]. Returning to the example of fluorescein, which exhibits weak photostability, this molecule can emit between 30,000 and 40,000 photons in water before photobleaching, and only a minor fraction of these will be collected during any experiment [44].

Although the photophysics and photochemistry associated with photobleaching are in general poorly understood, interactions between the fluorophore and molecular oxygen are thought to be one of the main causes for photoinactivation [92]. Upon transition of the fluorophore to long-lived triplet states (intersystem crossing), the molecule resides in the excited state for considerably longer periods of time (ms instead of ns), becoming considerably more susceptible to irreversible chemical reactions with oxygen and other molecules. Photobleaching can be partially reduced by oxygen depletion through the use of antifade agents composed of reactive oxygen scavengers or through the bubbling of N_2. Adding to the complexity of the phenomenon, oxygen is quencher of the triplet state and thus minimizes the lifetime of the reactive excited molecule. One possible consequence of oxygen depletion can be a drastic increase of the lifetime of the molecule in the dark triplet state, reducing the overall fluorescence as well [93]. In fact, other antifade agents make use of triplet-state quenching, reducing the reactivity of the dye.

Hence, particularly for fluorescence microscopy applications, fluorophores that exhibit strong photostability should be ideally chosen. While no rules exist for predicting the photostability of a dye [1], certain trends are observed, as within the same family of compounds, fluorophore elongation and flexibility are typically accompanied by less photostability [94]. The increased photostability of several Alexa dyes was obtained in part from rigidifying modifications of their structure [95]. Dyes with low degrees of triplet-state formation have also been associated with higher photostability [96].

As rhodamine-based dyes are frequently highly photostable, a large selection of these molecules is currently available from different companies with excellent properties. Several Alexa, DyLight, ATTO, HiLyte and Janelia dyes belong to this class and offer bleaching rates several fold lower than older generation dyes, such as fluorescein [81, 95, 97–99]. Improved photostability relative to fluorescein is also observed in boron–dipyrromethene BODIPY dyes [100]. The dyes presented above typically exhibit fluorescence between 450 and 700 nm, and when fluorophores emitting at shorter wavelength are required, coumarins are often used. However, coumarin derivatives are generally less photostable than rhodamine-based fluorophores. Examples of coumarin derivatives are Alexa Fluor 350 and

430, Marina Blue (Fig. 1), as well as ATTO 390, 425 and 465. Cyanine dyes such as from the Cy class, while extremely popular, are also not as photostable as most rhodamine-based derivatives, due to their susceptibility towards photooxidation [101]. On the other hand, very high photostability was also obtained with carbopyronines (e.g. ATTO 647) and oxazine derivatives (e.g. ATTO 655, ATTO 680 and ATTO 700) [102].

While photobleaching is almost always undesirable, in some cases, such as in fluorescence recovery after photobleaching (FRAP) or fluorescence loss in photobleaching (FLIP) experiments, photobleaching can actually be employed to study molecular diffusion rates [103, 104].

2.1.5 Aggregation and Solubility

An increase in labelling stoichiometry often does not necessarily lead to linear increases of fluorescence intensity, as probe self-quenching can reduce the quantum yield of conjugated fluorophores [83]. In some cases, significant intramolecular self-quenching can take place even at moderate ratios of dye to labelled molecule. As an example, in non-specific covalent labelling of proteins with Cy5, functionalization is favoured in the vicinity of already protein-bound Cy5 labels, leading to the formation of clusters of Cy5 within the protein [105]. As a result, a dramatic reduction of Cy5 quantum yield due to static self-quenching is observed even at rather low Cy5/protein ratios, causing multiple labelled proteins to exhibit even lower fluorescence than single-labelled proteins. This behaviour is due to the tendency of Cy5 for dimerization, giving rise to non-fluorescent complexes. This is less problematic for carbocyanines such as Alexa Fluor 647 and 4S-Cy5.5 which carry four sulfonate groups, as their presence increases repulsion between the dyes during conjugation [105, 106].

Dye aggregation is in fact a problem for most of the older generation of fluorophores, limiting the fluorescence of conjugates to coumarins, xanthenes and cyanines [95, 107]. The Alexa Fluor dyes correspond to sulfonated derivatives of fluorophores from these classes. The presence of sulfonated groups allows for reduced interactions during labelling and increased quantum yield of conjugates [95]. Additionally, sulfonation increases solubility of the dyes, allowing for conjugation in aqueous media, without the need for organic solvents.

2.1.6 Fluorescence Emission Spectra

The fluorescence emission spectra of commercially available fluorophores span the near ultraviolet (UV), visible (VIS) and near-infrared ranges (IR) of the electromagnetic spectrum. The choice of fluorophore to be used in a given fluorescence spectral range must of course take into consideration the detection restrictions of the equipment to be employed, such as limitations of filter combinations. The dramatic reduction in photon detection efficiency within typical photomultiplier detectors

above 700 nm [2] can also limit the range of useful probes to molecules emitting in the UV-VIS range. Additionally, experiments with biological samples often have to deal with the additional complexity created by the presence of autofluorescence, which is particularly strong in the UV range. These limitations regarding measurements in the UV and infrared are responsible for the popularity of fluorophores emitting visible light between 380 and 750 nm (Figs. 2 and 3).

Experiments with multiple fluorophores rely on accurate isolation of individual signals. This can be challenging in imaging applications heavily dependent on optical filters, as emission spectral overlap of multiple fluorophores can lead to contamination of the fluorescence signal from one molecule in the detection channel of another one (bleedthrough). In equipment with high spectral resolution, spectral acquisition can allow for separation of the signal from two fluorophores emitting in the same range of energies through the use of techniques such as spectral unmixing [38]. However, bleedthrough can be minimized using simply a judicious selection of probes guaranteeing minimal spectral overlap.

Fluorescent probes exhibiting narrow fluorescence emission spectra facilitate the procedure by increasing the spectral separation between coexisting dyes. While the use of narrow bandpass optical filters solves this issue, it also leads to recovery of only a fraction of the total fluorescence from a fluorophore with broad emission spectra. Organic dyes often display narrow fluorescence emission bandwidths, but there are many exceptions. While rhodamine-derived Alexa Fluor dyes and BODIPY derivatives show particularly narrow emission bandwidths, probes from the cyanine class are known for presenting broader emission [25, 39, 40].

One advantage of dyes with broad absorption and emission spectra is their greater versatility since they can be excited with different illumination sources and detected with different optical filter combinations.

Finally, employment of probes in the IR has some advantages. Simultaneous measurements with probes emitting in the UV-VIS range are possible with negligible bleedthrough. This is particularly important when simultaneous measurements with fluorescent proteins are desired, due to their broad emission spectra.

2.1.7 Stokes Shift

The separation between excitation and emission maxima of a fluorophore (Stokes shift) is critical for an efficient detection of fluorescence signal. When the fluorophore exhibits a larger Stokes shift, contamination of the detection with scattered excitation light is less likely and wider bandpass filters can be used for the detection of the fluorescence signal, improving sensitivity of the measurement. Hence, fluorophores with a larger Stokes shift are generally preferred. Large Stokes shift are observed in dyes with asymmetric structure and electron distribution [108]. However, most of the popular fluorophore classes already mentioned (xanthene, BODIPY and cyanine derivatives) present a rather small Stokes shift [108].

Another consequence of a short Stokes shift is the increase in overlap between excitation and emission spectra. As a result, fluorophores with a small Stokes shift are susceptible to homo-FRET events. Unlike typical FRET, where the donor is a chemically distinct molecule from the acceptor, in homo-FRET the donor and acceptor share the same structure. This is useful for detection of homo-oligomerization or clustering. BODIPY derivatives present particularly small Stokes shifts [53] and have been intensively employed in homo-FRET studies [109, 110].

2.1.8 Fluorescence Lifetime

The average time a molecule resides in the excited state following excitation is called fluorescence lifetime (τ). A very high lifetime is disadvantageous for imaging applications as it will correspond to a shorter number of excitation-emission cycles, reducing the number of photons acquired, and thus the fluorescence intensity. Most popular probes exhibit fluorescence lifetimes of 1–6 ns (Table 1). Notable exceptions are cyanine derivatives such as Cy5, which present fluorescence lifetimes lower than 1 ns [56], while pyrene has a characteristic long lifetime of hundreds of ns [43].

Fluorescence lifetime is independent of fluorophore concentration, allowing for highly robust measurements [1]. Analysis of protein interactions in living cells has benefited considerably from lifetime measurements, as FRET imaging by fluorescence lifetime does not require the extensive calibrations and image processing mandatory for intensity-based methods [104].

For some probes, this quantity is heavily dependent on the local environment of the fluorophore and can be used to sense its distribution or conformational changes of labelled macromolecules. Hoechst 33342 or ATTO 655 can be used to detect the presence of double-stranded DNA, as binding of the dyes to the double strand increases the lifetime of the excited state of these molecules (Table 1) [47, 51]. A DNA-binding BODIPY derivative was shown to detect protein–DNA interactions through fluorescence lifetime changes [111]. A similar BODIPY-based molecule with high mitochondrial affinity was employed to quantify mitochondrial membrane viscosity as its fluorescence lifetime increased concomitantly with reduced mobility in the membrane [112].

Fluorescence lifetime measurements can be carried out with a pulsed (time-domain) or modulated excitation sources [1]. When working with pulsed excitation, one must be aware that the fluorescence lifetime to be measured should be significantly shorter than the repetition rate of the laser. In Ti:Sapphire lasers, this value is limited to ~80 MHz, corresponding to a 12.5 ns interval between two pulses. In these conditions, in a sample with a fluorophore presenting a lifetime significantly longer than 3 ns, the sample will still have excited fluorophores immediately before a new pulse, generating an incomplete decay and an erroneous lifetime estimation [1]. For this reason, it is advised that the dye chosen for the fluorescence lifetime measurement should present lifetimes at least four times shorter than the laser repetition rate [113].

2.1.9 pH Sensitivity

As a rule, when choosing a fluorophore for a specific application which does not involve estimating pH, the fluorophore to be chosen should be pH insensitive. Although most commercially available probes are indeed pH independent, there are several notable exceptions, such as fluorescein itself. In fact, fluorescein signal exhibits a strong pH dependence, resulting from the phenolic pK_a of 6.4 [114]. Near neutral pH, the monoanionic form (ε = 29,000–32,600 M^{-1} cm^{-1}, QY = 0.36–0.37) exists in equilibrium with the dianion (ε = 76,900–87,600 M^{-1} cm^{-1}, QY = 0.92–0.95) [26]. Due to the photophysical differences between the two species, the fluorescence intensity of fluorescein is strongly dependent on pH, and when analysing data with fluorescein or fluorescein labelled conjugates, this must be considered. The proximity of the pK_a of fluorescein to the pH of most biological systems is detrimental for multiple applications. For this reason, several derivatives have been introduced, presenting modified pK_a values. Oregon Green, for example, presents a pK_a of 4.8, eliminating pH sensitivity in most biological systems [115].

On the other hand, the pH dependence of fluorescein also allows for the use of the fluorophore as a pH sensor. A fluorescent derivative of fluorescein introduced by Roger Tsien in 1982, 7′-bis-(2-carboxyethyl)-carboxyfluorescein (BCECF), presents a pK_a closer to 7 (6.98), more appropriate for sensing of intracellular pH [116, 117]. The additional carboxylations in this molecule decrease the membrane permeability of the dye significantly, reducing membrane leakage. Cellular loading of the dye can be carried out through the addition of acetoxymethyl (AM) ester groups to the fluorophore, which increase the permeability of the molecule but are hydrolysed by intracellular esterases, leading to intracellular accumulation. BCECF-AM is still one of the most popular intracellular pH sensors. When the goal is to measure pH within acidic compartments, such as lysosomes, then dyes with lower pK_a values can be employed.

2.1.10 Overview of Fluorescent Probe Classes

Coumarins

This family of compounds includes molecules containing the 2H-chromen-2-one motif and is arguably the largest among the small organic dye categories. Coumarins are usually very photostable, with high quantum yield and a very large Stokes shift [13]. Their blue emission makes them a good alternative for multi-colour imaging, being an easy combination for green-to-IR dyes. This excitation at short wavelengths can also be a drawback when imaging cells since it overlaps with autofluorescence. Coumarins also have limited brightness due to weak absorption (e.g. AF350 in Fig. 3) [13].

In any case, these fluorophores have been extensively used in life sciences during the past decades. In a recent example, π-extended fluorescent coumarin (PC6S) was

used to image lipid droplets through fluorescence lifetime imaging (FLIM), both in living cells and in the tissues of living mice [118]. Other alternatives, including caged derivatives with activation in the visible and near-IR spectral range, have also been explored. For example, diazocoumarin derivatives have been used to label protein in living cells in a selective and fluorogenic manner, upon photoactivation (uncaging) with visible or near-IR illumination [119].

Cyanines

In this category one can find the brightest fluorophores among organic dyes. Although cyanines usually present low QY ($\leq$0.25), they also have very high extinction coefficients (e.g. Cy5 in Figs. 3 and 4; Table 1) [13]. Cyanine derivatives contain conjugated polymethine chains with quaternary nitrogens in their chemical structure. Adjusting the functional groups and the length of the conjugated chains, the photophysical properties of the fluorophores can be largely tuned.

However, the use of cyanines can be limited by significant photobleaching, as previously discussed, and a small Stokes shift (possibly important for super-resolution microscopy approaches) [120, 121]. Additionally, Cy5 and Cy7 derivatives are easily oxidized in the presence of O_2 and O_3, preventing their use in experiments that require long measurement sessions [122]. The development of new derivatives with enhanced QY and increased oxidation resistance has mitigated these drawbacks.

Cyanines have been used in a great number of different applications. They even gained more relevance with the development of single-molecule localization microscopy (SMLM) techniques (see Sect. 4 below). More recently, cyanine probes have been used, for example, to detect and label mercury [123], DNA [124] and RNA [125] in living cells.

Fluorescein and Rhodamine-Based Dyes

As already mentioned, both fluorescein and rhodamines are xanthene dyes that have been extensively used since they were first synthesized [126, 127]. The reason of this wide popularity is associated mainly with their very high brightness and the fact that both excitation and emission wavelengths fall well within the visible spectral range. As previously described, with a pK_a value of 6.4, fluorescein spectral properties depend strongly on the environment pH (between 5 and 9). They can also present limited photostability [13, 122].

Over the years, numerous fluorescein and rhodamine derivatives have been developed, targeted at countless applications. Among the most commonly used fluorescein derivatives [128, 129] are fluorescein isothiocyanate (FITC), carboxyfluorescein, 5/6-carboxyfluorescein succinimidyl ester, fluorescein amidite (FAM) and fluorescein di-acetate. Rhodamine 6G, 110, 123 and rhodamine B are possibly within the most extensively used rhodamines, together with rhodamine-derived Alexa Fluor dyes. When used for live-cell imaging, properties like permeability, localization and aggregation state will strongly depend on the structural characteristics of each derivative.

BODIPYs

Boron dipyrromethene compounds or BODIPYs are very popular fluorophores due to their enhanced photophysical properties [130]. They present high quantum yields (e.g. BODIPY-TMR in Fig. 4), high brightness, sharp absorption and emission spectra and a very small Stokes shift (Table 1). Possibly the most significant limitation to the use of BODIPY dyes is their susceptibility to oxidation [13].

BODIPY variants included in this category cover a great portion of the visible spectrum, from green (BODIPY FL) to red (BODIPY 650/665). This versatility has been extensively explored through the development of BODIPY conjugates of different biomolecules, including proteins, lipids, lipopolysaccharides and nucleotides, among others. They have also been employed in live-cell imaging (see [131] for a comprehensive review). For example, BODIPYs have been recently used in the detection of hydrogen sulphide and lysosome tracking [132].

2.2 Methods for Fluorescent Protein Labelling

The choice of organic probe must always be performed hand-in-hand with the selection of the appropriate labelling strategy. The latter depends on the available fluorophore derivatives, the target molecule and the experimental requirements. Here, some of the most commonly used strategies for labelling proteins upon purification or within fixed or living cells are discussed (Fig. 5). The extensive description of these and other methodologies can be found in very thorough reviews elsewhere [133].

Covalent Binding to Natural-Occurring Amino Acids

The most common strategy to label purified proteins is to use fluorophore derivatives that directly react with amine groups or cysteine residues (Fig. 5) [134].

By using amine-reactive fluorophore conjugates, such as isothiocyanates or succinimidyl-esters, target proteins will be labelled in either lysine residues or the N-terminal amine. Due to the high frequency of lysine residues in proteins, labelling often results in the binding of several fluorophores at different positions, which can ultimately alter protein function and its possible interactions. Since lysine amine groups have significantly different *pKa* values than the terminal amine (*pKa* 10–11 versus *pKa* 7, respectively), it is possible to preferentially label the N-terminal [135]. Although this solves the issue of multiple labelling, it restricts the fluorophore position at the amino terminal.

Cysteine residues, on the other hand, are much less frequent in proteins and thus offer greater flexibility regarding the position of the fluorophore. In this case, maleimide fluorophore conjugates are used due to their high specificity for the cysteine thiol group [133]. In addition, the conjugation reactions are typically fast at mild pH and temperature.

Labelling amine groups or cysteine residues in intact cells or cell extracts is generally not feasible since it is not possible to reach labelling specificity under these

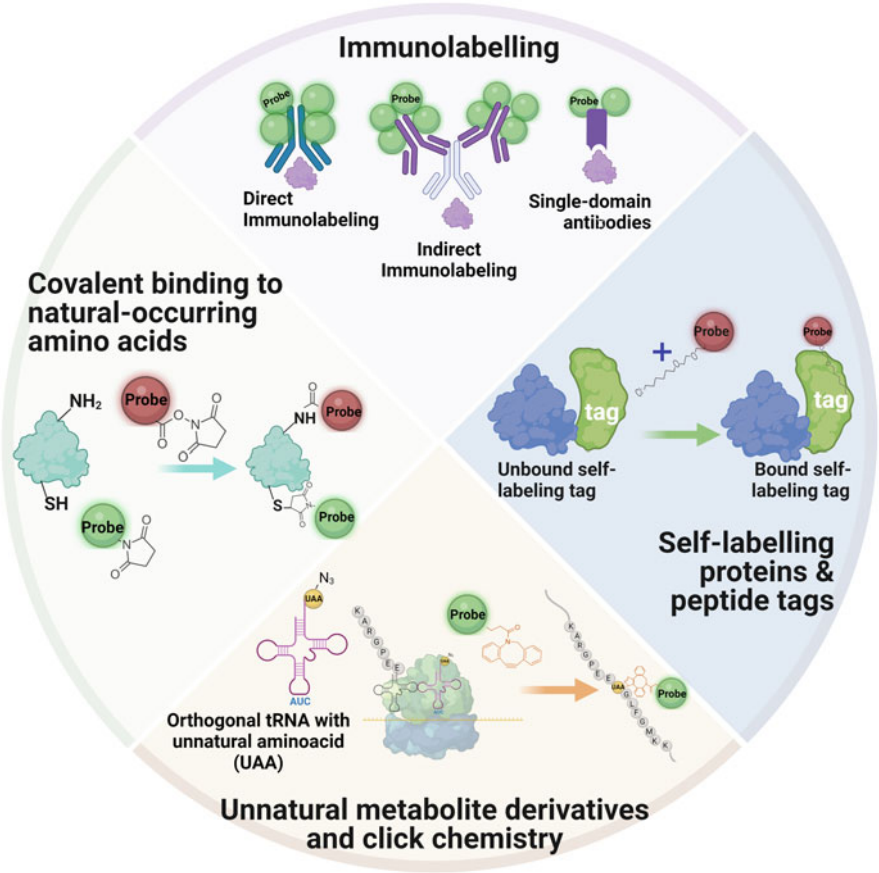

Fig. 5 Summary depiction of some of the most commonly used (or most promising) protein labelling methodologies. The examples depicted for covalent binding to natural-occurring amino acids are related to cysteine and protein amine labelling with maleimide and succinimidyl ester derivatives, respectively. The example portrayed for self-labelling proteins and peptide tags illustrates self-labelling by the HaloTag. The method shown below describes incorporation of an azide-containing unnatural amino acid (UAA) and site-specific labelling of the modified protein with Cu^{2+}-free click-chemistry. Figure created with BioRender (BioRender.com)

conditions. For this reason, these methods are more often employed for labelling of purified proteins.

Immunolabelling

To achieve high labelling specificity within cell samples, the classical approach is to use immunofluorescence [136]. In general, an externally added primary antibody specifically binds the target molecule/structure with high affinity. Subsequently, one or more secondary antibodies (conjugated with a fluorescent probe) form a stable complex with the primary antibody (indirect immunolabelling), allowing the specific

detection of the target (Fig. 5). Direct immunolabelling with one labelled specific antibody is also possible. However, antibodies are large molecules of ~150 kDa and thus their use implies a couple of limitations [137]. First, they cannot cross the plasma membrane, limiting their application to fixed, and thus, dead cells. This prevents the study of dynamic processes, providing only a snapshot of the target molecule at the time of fixation. Also, it is important to keep in mind that the fixation protocol itself might interfere with the observed cell morphology and/or the properties of the molecule of interest. Second, the size of the antibodies and that of the antibody complex (primary + secondary) makes it so that the detection system is often much larger than the target molecule or structure [137]. In this case, determination of the target's size becomes extremely difficult and, for example, molecules that are well far apart might look closer or even interacting when immunolabelled. Importantly, this might have serious implications in single-molecule localization microscopy techniques, with the location of the fluorophore possibly being clearly distinct from that of the target molecule.

More recently, these limitations have been overcome by the development of single-domain antibodies (sdAbs) or 'nanobodies' [138–140]. sdAbs are much smaller (~15 kDa) than traditional antibodies, highly stable and soluble in many environments. Depending on the experimental requirements, sdAbs can even be functionalized, for example, to cross the plasma membrane and allowing live-cell imaging. Their smaller size also makes them much better suited to help evaluate the dimensions of biological structures, as opposed to the traditional antibodies.

Self-labelling Proteins & Peptide Tags

Possibly the most widely used strategy to label proteins with synthetic probes inside living cells is the use of small self-labelling proteins or tags (<40 kDa) [141]. In this approach, the target protein is expressed as a fusion construct containing a polypeptide or protein designed to react with a fluorescent probe (or other moieties such as biotin) via a specific biorthogonal reaction. This ensures the covalent binding of virtually any fluorescent probe to the protein of interest as long as the proper biorthogonal functionalization of the probe is available and compatible with the particular self-labelling protein to be used. The versatility of this method is also increased by the number of tags that have already been developed (derived from different proteins): HaloTag (derived from the haloalkane dehalogenase) (Fig. 5) [142], SNAP-tag (derived from human O6-alkylguanine DNA alkyltransferase) [143, 144], CLIP-tag (derived from SNAP-tag) [145], DHFR-tag (derived from dihydrofolate reductase) [146], BL-tag (derived from b-lactamase) [147], PYP-tag (derived from the photoactive yellow protein in purple bacteria) [148] and RA-tag (derived from de novo designed retroaldolase) [149].

Ideally, the tags should be as small as possible to avoid interfering with the target protein, should present low substrate promiscuity, fast labelling kinetics and thermodynamic stability. The main advantages of this approach are associated with the use of synthetic dyes (described above) and their superior photophysical performance, and yet being genetically encoded, thus offering a better control over the degree of labelling. Moreover, it can be used for pulse-chase assays, contrary to FPs

[150]. The disadvantages, however, also stem from the fact that the tags are genetically encoded. First, this means that the labelling is restricted to the N- or C-termini, preventing any site-specific tagging into internal regions of the protein of interest [74]. Second, the tags are still proteins with diameters that can reach 3–4 nm, comparable to that of FPs [35, 74]. The labelling can thus affect the folding, location and function of the native target protein.

Alternatively, a tetracysteine peptide can be genetically introduced into the protein of interest (not necessarily at the termini), instead of the self-labelling protein [151]. The peptide sequence, Cys-Cys-X-X-Cys-Cys (where X is any amino acid apart from cysteine), is then able to specifically react with membrane-permeable biarsenical dyes. The standard biarsenical dyes in use are FlAsH-EDT_2 (fluorescein arsenical hairpin binder) and ReAsH (resorufin arsenical hairpin binder) that emit in the green and red regions of the spectrum, respectively [35]. Although the tetracysteine peptide shares most of the advantages with the self-labelling proteins, the major point of differentiation is their size. In this case, the much smaller size of the moiety is less likely to interfere with the conformation and function of the protein of interest. Nevertheless, the use of biarsenical dyes can still perturb the protein's native conditions, can lead to considerable levels of background fluorescence and might induce some cytotoxicity.

Unnatural Metabolite Derivatives & Click-Chemistry

More recently, specific molecular labelling within the cellular environment has been accomplished through the development of the so-called click-chemistry (Fig. 5). Contrary to genetically encoded reporters, it can be used to label not only proteins but also other biomolecules such as DNA, lipids and glycans. This labelling strategy is a two-step process. First, cells must be cultured in the presence of non-natural metabolites with a 'clickable' moiety [12]. For example, nucleotides BrdU (5-bromouridine) and EdU (5-ethynyl-2′-deoxyuridine) have been used to tag nascent RNA and DNA, respectively [152]. Then, fluorescent labelling is accomplished through a biorthogonal 'click' reaction with probe derivatives containing the corresponding 'click' feature (e.g. azide or alkenyl groups). In the case of EdU, azide Alexa Fluor derivatives are commonly used. The most typical biorthogonal reaction is named azide-alkyne cycloaddition, requires copper [Cu(I)] as catalyst and has the main advantages of being fast, regioselective and presenting high yields [153, 154]. However, due to copper cytotoxicity, other alternatives have also been widely employed [155]. These copper-free reactions include the azide-alkyne cycloaddition between an azide and a strained cyclooctyne [156] and the Staudinger ligation between an azide and a phosphine [157]. Although the copper-free character of these reactions makes them uniquely suited for in vivo labelling, they tend to be less efficient, meaning that the reaction time might need to be increased to assure full conjugation of the fluorescent probe derivative with the unnatural metabolite [158]. In any case, when planning an experiment, the choice of reaction will greatly depend on the system, the target biomolecule and the technique to be employed [12]. Moreover, copper toxicity, alterations of membrane permeability and possible background fluorescence must also be considered.

When considering labelling proteins using 'click-chemistry', a promising strategy has recently emerged that combines genetically encoded site-specific labelling with the major advantages of using small synthetic dyes. This is accomplished through the use of unnatural amino acids (UAAs) that can either be conjugated with an organic probe via a biorthogonal reaction (Fig. 5) or be already incorporated as a fluorescent amino acid derivative [159, 160]. UAAs, also called the expanded genetic code, are molecules that are not found in native proteins, but were rather discovered in nature or chemically synthesized [161–163]. Examples include selenocysteine (Sec) and pyrrolysine (Pyl), also referred to as the 21st and 22nd amino acids [164]. In principle, many other UAAs can (and some have been) incorporated into target proteins by using a nonsense codon and the UAA respective orthogonal pair [165]. This strategy confers large flexibility when it comes to the labelling position within the target protein, with the advantage of keeping the labelling ratio under control (since it is genetically encoded). Also, due to their much smaller size, UAAs overcome most issues related to the interference with the native protein, as discussed above for self-labelling proteins. Yet, incorporation of UAAs (and their fluorescent labelling) is still challenging [74, 166, 167] and there is still some work to be done to make it the method of choice for live-cell protein labelling.

2.3 Membrane Probes

Fluorescence microscopy and spectroscopy are invaluable tools for the imaging and characterization of cellular membranes or membrane model systems. Membrane staining can be achieved through labelling of specific targets (e.g. glycoproteins and glycolipids with wheat germ agglutinin (WGA) conjugates [168]), with derivatized membrane components (e.g. labelled cholera toxin-A or BODIPY-labelled phospholipids, or through simple partitioning of lipophilic dyes [1]. This section will focus solely on probes of the latter class.

Lipophilic staining of cellular membranes is often employed in cell imaging applications. Lipophilic carbocyanines with hydrocarbon tails, such as DiO (green fluorescence), DiI (red fluorescence), DiD (far-red fluorescence) or DiR (near-infrared fluorescence), are particularly popular for this application [169, 170]. Styryl dyes such as FM4–64 or FM1–43 also belong to the class of lipophilic stains. Unlike lipophilic carbocyanines, these dyes are not lipophilic enough to translocate across the lipid bilayer and become anchored to the outer leaflet of the plasma membrane, with minimal translocation to the cytoplasmic leaflet [171]. This property leads to their popularity as tools for evaluation of intracellular vesicle trafficking [171, 172]. FM4–64 is generally preferred to FM1–43 as it is brighter and more photostable. FM4–64 also allows for simultaneous imaging with green emitting dyes and fluorescent proteins as it exhibits red-shifted fluorescence [171]. All these dyes

benefit greatly from the fact that their quantum yield is close to zero in water, thus generating better staining contrast.

Beyond the simple staining of lipid membranes, lipophilic fluorescent membrane probes can provide important information on membrane structure. The time scale of fluorescence is adequate to the analysis of fluorophore dynamics during the excited state and solvent-dependent excited-state relaxation [173, 174]. In turn, information about these processes allows us to evaluate membrane viscosity and lipid packing.

Membrane viscosity has been shown to regulate the activity of several membrane proteins and is linked to multiple physiological processes within the cell [175]. Lateral diffusion can be quantified through measurement of the diffusion coefficient of fluorescent membrane components using fluorescence recovery after photobleaching (FRAP) [176] or fluorescence correlation spectroscopy (FCS) [177]. On the other hand, local dynamics within the membrane can be evaluated through the use of fluorescent microviscosity probes.

DPH (1,6-diphenyl-1,3,5-hexatriene) and its trimethylamino-derivative, TMA-DPH are part of a class of membrane viscosity probes whose fluorescent polarization/anisotropy is strongly dependent on local microviscosity [178, 179]. The DPH fluorophore only absorbs light polarized along its long axis and the polarization of emitted photons has the same orientation [180]. In this way, rotation of the fluorophore (during its excited state) along its long axis has no impact on the polarization of fluorescence, while rotation along the two perpendicular axes induces depolarization [179]. As acyl-chain fluctuations dictate rotation of the fluorophore during its excited state, fluorescence anisotropy values of these dyes reflect local membrane viscosity. Due to the presence of the trimethylamino-derivative, TMA-DPH becomes anchored to the lipid–water interface and reflects viscosity in a slightly more shallow region of the lipid bilayer [178]. Another useful membrane probe sensitive to membrane viscosity is trans-parinaric acid (*t*-PnA) [181]. The fluorescence lifetime of *t*-PnA is strongly dependent on membrane dynamics, and the appearance of a very long lifetime (>30 ns) is used as a fingerprint for the presence of gel phase membrane domains [179, 182, 183]. Finally, a class of molecules known as molecular rotors, which include 9-(dicyanovinyl)-julolidine (DCVJ), 9-(2-carboxy-2-cyano)vinyl julolidine (CCVJ) and BODIPY-C_{12} present fluorophores with the ability of twisting along a single bond. This movement is hindered within ordered membranes influencing fluorescence properties such as quantum yield or fluorescence lifetime [184, 185].

Polarity sensitive probes such as 2-dimethylamino-6-1auroylnaphthalene (Laurdan) can also be used to evaluate membrane packing, as these dyes exhibit strong spectral changes upon changes in membrane ordering [65, 186]. One advantage of Laurdan and similar probes is that membrane order can be estimated from simple ratiometric measurements reflecting spectral shifts, facilitating their implementation in imaging applications.

3 Fluorescent Proteins

Fluorescent proteins (FPs), more precisely the green fluorescent protein (GFP) was discovered in 1962 [187]. Since then, the use of FPs in life sciences has been at the centre of a great and unparalleled revolution in the way we 'see' cellular events at the molecular level. Unsurprisingly, 'the discovery and development of the green fluorescent protein' earned Osamu Shimomura, Martin Chalfie and Roger Tsien the Nobel Prize in Chemistry in 2008, unequivocally stating the importance of such finding for modern science and medicine.

GFP is a 27 kDa protein from the jellyfish *Aequorea victoria* that folds into a β-barrel structure where three sequential amino acids (Ser-Tyr-Gly in positions 65–67) form the protein chromophore upon cyclization, oxidation and dehydration steps, without the need for enzymes or cofactors [16, 188]. The main reason for GFP popularity from the start is associated with the advantage of being genetically encoded, thus bypassing many problems associated with the use of synthetic probes for protein labelling. Namely, their use avoids mis(or multi)labelling of proteins, issues with background fluorescence due to unspecific binding and is also completely compatible with live-cell (and tissue) imaging. Moreover, engineering a fusion construct is relatively easy at the experimental level, being routinely performed in many laboratories.

Although GFP is still frequently used, many other variants with different and improved photophysical properties are now widely available (Table 2). These variants were either discovered in other organisms such as sea anemone [216], copepod [216] and lancelet [217], or developed through the modification of the original protein barrel structure by mutagenesis. Many modifications in the core chromophore structure were performed [206], as well as changes in the side chains of nearby amino acids [16, 218]. The result is a large variety of FPs of different colours (from violet to far-red) covering almost entirely the visible spectrum. Moreover, the development of FPs with large (>100 nm) Stokes shift [219–222], and the possibility of generating tandem FP versions apart from the monomeric ones [223, 224] further increase the number of available choices. Yet, attempts are continuously being made to develop different FPs with, among other features, improved brightness, with other excitation/emission wavelengths and enhanced pH resistance (when compared with the original proteins). The engineering of red fluorescent proteins (RFP) has also been the focus of numerous attempts since they would present a few additional advantages. As already described for organic probes, fluorescence in the red to near-infrared region of the spectrum ensures a more efficient tissue penetration, decreases any issues related to cell autofluorescence and, additionally, relieves some of the spectral crowding (and consequent channel bleedthrough) usually encountered when designing multi-colour imaging experiments. DsRed from *Discosoma* was the first RFP to be isolated [225]. However, this protein shows severe limitations that precluded its generalized use. DsRed assumes a GFP-like intermediate form during maturation and a fraction of the protein exhibits excitation in the green spectral region. Furthermore, it requires over 30 h of

Table 2 Overview of the most commonly used fluorescent proteins, their oligomerization state and main photophysical properties

Protein	Oligomerization	ε (M^{-1} cm^{-1})	$\lambda_{max,abs}$ (nm)	$\lambda_{max,em}$ (nm)	QY	Brightness ($\times 10^3$ M^{-1} cm^{-1})	References
TagBFP	Monomer	52,000	402	457	0.63	33	[189]
mTurquoise	Monomer	30,000	434	474	0.93	28	[190]
MCerulean3	Monomer	40,000	433	475	0.87	35	[191]
EGFP	Weak dimer	55,900	488	507	0.6	34	[192]
rs-EGFP	Monomer	47,000	493	510	0.36	17	[193]
Skylan -NS	Monomer	133,770	499	511	0.59	79	[194]
T-Sapphire	Weak dimer	44,000	399	511	0.6	26	[195]
mGreenLantern	Monomeric	102,000	503	514	0.72	73	[196]
mNeonGreen	Monomer	116,000	506	517	0.8	93	[197]
PA-GFP	Monomer	17,400	504	517	0.79	14	[198]
mClover3	Monomer	109,000	506	518	0.78	85	[199]
rsFastLime	Tetramer	39,094	496	518	0.77	30	[200]
mAmetrine	Monomer	45,000	406	526	0.58	26	[201]
EYFP	Weak dimer	67,000	513	527	0.67	45	[202]
mVenus	Monomer	104,000	515	527	0.64	67	[203]
mCitrine	Monomer	94,000	516	529	0.74	70	[204]
mOrange	Monomer	71,000	548	562	0.69	49	[205]
tdTomato	Tandem dimer	138,000	554	581	0.69	95	[205]
DsRed	Tetramer	75,000	558	583	0.68	51	[206]
rsTagRFP	Monomer	36,800	567	585	0.11	4	[207]
mApple	Monomer	75,000	568	592	0.49	37	[208]
mRuby3	Monomer	128,000	558	592	0.45	58	[199]

mScarlet	Monomer	100,000	569	594	0.7	70	[209]
PamCherry	Monomer	18,000	564	595	0.46	8	[210]
PATagRFP	Monomer	66,000	562	595	0.38	25	[211]
mCherry	Monomer	72,000	587	610	0.22	16	[205]
mKeima	Monomer	14,400	440	620	0.24	3	[212]
PamKate	Monomer	25,000	586	628	0.18	5	[213]
mKate2	Monomer	62,500	588	633	0.4	25	[214]
mNeptune	Monomer	67,000	600	650	0.2	13	[215]

incubation time at 37 °C to achieve steady-state levels and, since it is an obligate tetramer, it might force tetramerization of any target protein [226–228]. For these reasons, additional efforts have been carried out to bioengineer new and better performing RFP. Yet, despite considerable advances, the photophysical properties of RFPs still fall short when compared with the performance of other FPs.

FPs have been employed in the study of an immense number of cellular functions and processes. These have been extensively reviewed elsewhere [229–231]. However, it is worth noting that FPs are particularly well suited for the development of biosensors, allowing the imaging and quantification of diverse cellular processes [232]. Briefly, there are mainly four classes of FP-containing biosensors: (1) FPs with environment-dependent photophysical properties (e.g. brightness or emission wavelength) that detect changes in pH [233], Cl^- [234], metal ions [235] and redox potential [236], among others; (2) FP-target constructs where the photophysical properties of the FP are affected by conformational changes in the target protein and that have been used, for example, to detect hydrogen peroxide [237] and membrane potential variations [238]; (3) Sensors in which detection relies on differences in the FRET efficiency between two spectrally distinct FPs [239]. FRET sensors were already applied to the detection of Ca^{2+} [240], cyclic nucleotides [241] and others; (4) FP-target constructs used as translocation sensors [242]. In other words, when linked to specific target proteins, FPs can report on environmental changes in intercellular compartments.

When expressing FP-containing fusion constructs, a fine balance must be accomplished. The expression level should not be so high that would interfere with cell functioning but should at the same time be high enough to allow a proper fluorescence signal for cell imaging purposes [12]. It is also important to take into account the maturation speed of the chromophore and the possible aggregation of the construct [243]. In extreme cases, this can affect the folding of the FP and consequently the structure of the chromophore itself, thus compromising the fluorescence output of the protein [244]. Depending on the experimental design, optimization of the nucleotide sequence for a particular model organism might also be required [245, 246], as well as the fine-tuning of the length and flexibility of the linker peptide between the FP and the target protein [247, 248].

Despite the wide-ranging use of FPs in cell biology and imaging, this technology still poses some limitations [249]. The most well-known is arguably their size (2–5 nm), which means that in some studies the size of the FP is comparable to that of the target protein, thus preventing, for example, the precise localization of the protein of interest. For the same reason, there is always a chance that the FP not only interferes with the subcellular localization of the target but also impairs the protein's biological function [250]. This is even more important when the initial FP variants are considered since they show a significant tendency to dimerize [251, 252]. This however has been mitigated or completely eliminated in newer FPs through the replacement of hydrophobic amino acids at the surface for positively charged amino acids [204]. Among the disadvantages are also the limitation of labelling at the protein terminals, loss of FP fluorescence upon fixation [253] or brightness dependence on the expression and maturation temperature for some FPs [254]. Moreover,

at the single-molecule level, FPs are known to blink at all timescales. Despite being associated with triplet and radical states, blinking of some variants has been related to proton transfer and conformational dynamics, involving different states of the chromophore [255]. Still, in many applications blinking is not a problem, but should be considered at the experiment design stage.

Apart from the issues discussed above, selection of an FP for an experiment should also involve the evaluation of the same properties previously discussed for organic dyes. Some of these are summarized in Table 2.

4 Fluorescent Probes for Super-Resolution Microscopy

Super-resolution microscopy surpasses the diffraction barrier by precluding the simultaneous signalling of adjacent fluorophores. In general terms, this is accomplished by transiently or permanently transferring (switching) fluorophores between two distinguishable states with different spectral, temporal or other detectable response to illumination. The choice of proper fluorophore is thus a requirement to achieve the best possible resolution. Although all the selection criteria described in the sections above still apply here, photophysical parameters such as brightness, photostability and switching kinetics gain additional relevance, depending on the chosen imaging technique. Super-resolution approaches have been thoroughly reviewed elsewhere [256–258].

In single-molecule localization microscopy (SMLM) [259], for example, only a subset of sparse fluorophores gets activated at any given time, allowing the accurate determination of the fluorophore's position with sub-diffraction precision. By repeating the process several times, exciting stochastically different molecules, it is therefore possible to reconstruct an image combining all the determined positions. Choosing photoactivatable fluorophores for SMLM should then consider the fluorescence contrast between *on* and *off* states, the turn-*on* halftime, the photobleaching halftime and the photon yield of individual molecules before bleaching [218, 260, 261]. Desirably, the photon yield should be high not only to ensure accurate position determination but also to allow the use of lower laser power. In case of reversible *on*/*off* switching, it is also important to take into account the number of photons detected per switching event, the *on*/*off* duty cycle (fraction of time a fluorophore spends in the fluorescent versus non-fluorescent state), the fatigue resistance (number of switching cycles required to bleach 50% of the initial fluorescence) and the fluorophores' survival fraction after subjected to relatively severe conditions [260]. To ensure the required sparse activation of fluorophores, the *off*-switching (or bleaching) rate must be much larger than the *on*-rate, resulting in a low duty cycle between 10^{-4} and 10^{-6} [262, 263].

In a very distinct approach, stimulated emission depletion (STED) microscopy overcomes the diffraction limit by reversibly silencing fluorophores at predefined positions within the diffraction-limited point-spread function (PSF) [264]. The excitation light is combined with a high-intensity doughnut-shaped laser that depletes

Table 3 Summary of the photoswitchable fluorescent proteins most commonly used for super-resolution microscopy, their oligomerization state, colour transition and photophysical properties of both states

Protein	Oligomerization	Transition[a]	ε (M^{-1} cm^{-1})	$\lambda_{max,abs}$ (nm)	$\lambda_{max,em}$ (nm)	QY[b]	References
Dendra2	Monomer	G/R	45,000/35,000	490/553	507/573	0.5/0.55	[277]
Kaede	Tetramer	G/R	98,800/60,400	508/572	518/580	0.88/0.33	[278]
mClavGR2	Monomer	G/R	19,000/32,000	488/566	504/583	0.77/0.53	[279]
mEos3.2	Monomer	G/R	63,400/32,000	507/572	516/580	0.84/0.55	[280]
mIrisFP	Monomer	G/R	47,000/33,000	486/546	516/578	0.54/0.59	[281]
mMaple3	Monomer	G/R	15,760/23,970	491/568	506/583	0.37/0.52	[263]
NijiFP	Monomer	G/O	41,100/42,000	469/526	507/569	0.64/0.65	[282]
PS-CFP2	Monomer	C/G	43,000/47,000	400/490	468/511	0.2/0.23	[283]
PSmOrange	Monomer	FR/O	32,700/113,300	634/548	662/565	0.28/0.51	[284]

[a] *G/R* green-to-red, *G/O* green-to-orange, *C/G* cyan-to-green, *FR/O* far-red-to-orange
[b] Quantum yield

fluorescence in specific regions (doughnut-shaped periphery) while leaving a central focal spot active. The acquisition is performed by scanning the sample with the two aligned beams and, by making so, only the non-silenced fluorophores in the central complementary regions emit light. As a consequence of this setup, fluorophores for STED microscopy must be quite photostable and thus exhibit high resistance to photobleaching [265–268]. Additional criteria for fluorophore selection include: (1) the emission spectrum of the fluorophore must be compatible with the available STED laser to be used [269]; (2) spectral overlap between stimulated emission and excited-state absorption should be avoided [265]; (3) large Stokes shift probes should be preferred to prevent direct excitation of the fluorophore by the STED beam and also to assist in multi-colour imaging [265, 270, 271]. However, most of the available large Stokes shift probes still do not present the required high brightness and enhanced photostability [265].

Although this description of SMLM and STED is not meant to be extensive, it is clear from these examples that the choice of super-resolution technique determines the fluorophore to be used. As for conventional imaging, many different types of fluorophores were already applied to one or several super-resolution approaches, including small organic probes [73], fluorescent proteins [272], quantum dots [273] and nanoparticles [274], among others. Moreover, fluorophores that use reversible ligand binding [275] or quenching [276] as a switching mechanism instead of photoswitching have also been employed. In the next sections, the most common classes of switching organic probes and FPs (Table 3) are briefly introduced, including some recent examples of their application. Detailed information on their mechanism and performance can be found elsewhere [218, 260, 285].

4.1 Synthetic Probes

Activator-Reporter Dye Pair

This system consists of a ‘reporter’ probe that switches between a fluorescent and a dark state and whose photoactivation is facilitated by an ‘activator’ fluorophore placed within 1–2 nm distance [218]. The ‘reporter’ dye is usually kept in a non-fluorescent state, and the random activation of non-overlapping fluorophores is accomplished by the use of an activation laser that excites the ‘activator’ probe. The ‘activator’ can then induce its ‘reporter’ neighbours to become fluorescent. The final image is consequently reconstructed from emission signal of the ‘reporter’.

The first system to be described was the Cy3-Cy5 combination, used by Xiaowei Zhuang to develop stochastic optical reconstruction microscopy (STORM) [286]. Since then, several combinations of ‘activator’ dyes (e.g. Cy2 or Alexa Fluor 405) and ‘reporters’ (e.g. Cy5.5, Cy7 or Alexa Fluor 647) were employed [287, 288].

Activator-Free Dyes

Some dyes are stochastically activated in the absence of an activator fluorophore and under continuous laser illumination [218, 289]. However, they frequently require significantly higher laser power. The switching behaviour also entails a specific chemical environment. For this reason, the imaging buffers usually include 'non-common' components such as triplet quenchers, oxygen scavengers, reducing agents and others [290–293].

These dyes were first applied by Sauer and co-workers to perform direct STORM [97, 289]. In this pivotal work, the authors used cyanine dyes (without 'activators') that could be photoswitched under reducing conditions [289]. Recently, a comprehensive study compared the performance of 26 commercially available probes in a STORM setup and identified the best-performing dyes in different colour ranges: Atto488 for the green spectral region, Cy3B for the yellow, Alexa Fluor 647 for the red and DyLight750 in the near IR [260].

Spontaneously Blinking Dyes

Contrary to the probes from the categories described above, spontaneously blinking dyes do not need activators or incident light to become active. Instead, they spontaneously blink in the absence of light in a stochastic and reversible manner [218]. Spontaneously blinking dyes often switch between an 'open' fluorescent state and a 'closed' dark state. One such example is the intramolecular spirocyclization that occurs in hydroxymethyl (HM) rhodamines, from which other related derivatives have been developed. Hydroxymethyl-Si-rhodamine (HM-SiR) [294] and HEtetTFER [295], for example, have been applied to SMLM by Yasuteru Urano and his team, allowing the use of reduced illumination intensities and still presenting a high photon yield. In a different approach, Urano's team also described a different spontaneous blinking mechanism that relies on the reversible ground-state nucleophilic attack of intracellular glutathione (GSH) upon a xanthene fluorophore [296]. This allowed the observation of microtubules and mitochondria within living cells by SMLM. Although not many options are available so far, the recent developments in this area suggest an increase in the use of these dyes in the coming years.

Photochromic Dyes

Fluorophores that switch reversibly between an *on* and *off* state in a light-assisted manner are called photochromic [218]. These include different rhodamines, diarylethenes and photoswitchable cyanines [297]. Rhodamine lactams, for example, are colourless compounds that become fluorescent through the transient cleavage of the lactam bond upon far-UV illumination [298]. The fluorescent molecule then thermally reverts back to its non-emissive state. This reversible photoswitching mechanism is well suited for SMLM and efforts have been made to extend it to other rhodamines with different photophysical properties. Moreover, the addition of different substituents to the rhodamine core has also led to the development of photochromic dyes with activation light that is not in the far-UV spectral range. Phthalimide groups were shown to allow for near-UV (or 2-photon) activation [299] while stilbene groups even made it possible to use visible light [300, 301]. One of

such examples are the 'turn-on mode' fluorescent diarylethenes (fDAEs) recently developed by the Hell group. With yellow light activation, fDAEs were successfully applied to the visualization of cells' vimentin filaments by SMLM [302].

Photoactivatable or 'Caged' Dyes

In contrast to the photochromic probes, 'caged' dyes are irreversibly activated through a photochemical reaction [218]. These molecules combine fluorophores with photolabile (or caging) moieties located at appropriate positions that block them in a non-emissive state. Upon illumination, the protective groups are either removed or modified and the fluorescence emission of the dye is greatly increased [137, 262]. The use of caged dyes thus results in great *on*/*off* contrast and photon yield [218], making them ideal for SMLM techniques such as photoactivated localization microscopy (PALM) [303] and DNA points accumulation in nanoscale topography (DNA-PAINT) [304]. The photoactivation quantum yield can however be a critical element to consider.

Among the most common caging moieties are the o-nitrobenzyl derivatives, azides, coumarinyl groups and 2-diazoketones [305]. Different fluorophores have also been successfully caged, such as Q-rhodamine [303], rhodamine 110 [306], Si-Q-rhodamine [99], carbofluorescein [307], and several others.

4.2 Fluorescent Proteins

Photoactivatable (PA-FPs)

This category includes proteins that are irreversibly switched from a non-fluorescent *off*-state to a fluorescent *on*-state upon illumination. The development of PA-FPs goes hand-in-hand with the establishment of SMLM techniques. Indeed, PA-GFP (developed by Patterson and Lippincott-Schwartz [198]) was used in the very first papers on PALM [308, 309]. Due to its photophysical properties, high activation quantum yield and their monomeric state, PA-GFP is still one of the most used and dependable PA-FPs. Since then, several other variants were developed, including the ones within the orange/red spectral range, such as PAmRFP, PAmCherry, PATagRFP and PAmKate.

Nevertheless, the use of PA-FPs makes it hard to detect cells expressing the protein, since before illumination they remain in a non-fluorescent state [218]. This drawback is largely overcome by the use of photoswitchable dyes instead (see below).

Photoswitchable (PS-FPs)

Photoswitchable (or photoconvertible) FPs rely on the irreversible conversion from one fluorescent *on*-state to another of a different colour [285]. Depending on the specific colour transition, PS-FPs can be categorized as (1) GFP-like cyan-to-green proteins (PS-CFP2), (2) Kaede-like green-to-orange/red proteins (Dendra2, mEos3.2, mClavGR2, mMaple3) or (3) DsRed-like green-to-far red proteins (PSmOrange). This spectral coverage together with the photoswitching capability

makes them not only ideal for simple SMLM experiments but also allows their use in multi-colour super-resolution imaging.

Although extensively applied, it is worth noting that even the brightest PS-FP remains much dimmer than some organic probes, with photon yields that can be one order of magnitude lower (e.g. comparing Eos with the Cy3-Cy5 pair) [287, 310, 311].

Photochromic (PC-FPs)
As their small-molecule counterparts, photochromic FPs are able to reversibly transition between a dark *off*-state and a fluorescent *on*-state. However, their main advantage over photochromic organic probes is the stability and reliability of their switching system, meaning that they are much more resistant to switching fatigue [262]. This also explains the use of these proteins in non-linear super-resolution imaging approaches such as non-linear structured-illumination microscopy (NL-SIM) [312] or reversible saturable optical fluorescence transition (RESOLFT) [313]. Examples of PC-FPs include rs-EGFP, rsFastlime, rsTagRFP or Skylan-NS.

Photoactivatable/Photoconvertible FPs
This category includes proteins with complex working mechanisms that combine the photoswitching behaviour of PC-FPs and PS-FPs. In other words, proteins such as mIrisFP [281] and NijiFP [282] can be irreversibly photoconverted between two *on*-states (green-to-red transition) and then feature a reversible photoswitching behaviour from both species to a dark *off*-state. Due to their complicated mechanism, these are the only FP variants included in this category.

5 Perspectives

Researchers in the field of biological sciences have now available an enormous abundance of different fluorescent probes to choose from. These present remarkably diverse properties so that specific experiments can make use of ideally suited labels. There are however still some limitations that are expected to be addressed. When it comes to organic dyes, significant difficulties still limit the ability to specifically label target molecules within a living cell or tissue. The next years will undoubtedly bring new and creative strategies combining biorthogonal chemistry with the use of unnatural metabolites and caged dyes, to achieve the required labelling specificity in a live-cell compatible manner. Regarding FPs, researchers are still paving the way to improve their photophysical properties and overall performance. Although they show the ultimate labelling specificity, there is still room for improvement in terms of FP photostability and brightness, to reduce the performance gap that remains when comparing FPs with synthetic dyes. In any case, whether it is organic dyes or FPs, the development of photostable, highly performing far red to near-IR probes is arguably one of the biggest challenges of the next years.

Overall, the available fluorescent probes used for life sciences cover already a very wide spectrum of applications. Nonetheless, the design of new probes must

continue to walk hand-in-hand with the development of new techniques and approaches, as were the case of super-resolution microscopy and the development of photoswitchable fluorescent probes.

References

1. Lakowicz JR (2006) Principles of fluorescence spectroscopy. Springer, Boston
2. Andersson H, Baechi T, Hoechl M, Richter C (1998) Autofluorescence of living cells. J Microsc 191:1–7
3. Monici M (2005) Cell and tissue autofluorescence research and diagnostic applications. Biotechnol Annu Rev 11:227–256
4. Brandes R, Bers DM (1996) Increased work in cardiac trabeculae causes decreased mitochondrial NADH fluorescence followed by slow recovery. Biophys J 71:1024–1035
5. Masters BR, Chance B (1999) Redox confocal imaging: intrinsic fluorescent probes of cellular metabolism. In: Fluorescent and luminescent probes for biological activity. Elsevier, pp 361–374
6. Hellmann N, Schneider D (2019) Hands on: using tryptophan fluorescence spectroscopy to study protein structure. In: Protein supersecondary structures. Humana Press, New York, pp 379–401
7. Vivian JT, Callis PR (2001) Mechanisms of tryptophan fluorescence shifts in proteins. Biophys J 80:2093–2109
8. Royer CA (2006) Probing protein folding and conformational transitions with fluorescence. Chem Rev 106:1769–1784
9. Ghisaidoobe ABT, Chung SJ (2014) Intrinsic tryptophan fluorescence in the detection and analysis of proteins: a focus on förster resonance energy transfer techniques. Int J Mol Sci 15: 22518–22538
10. Banerjee B, Graves LR, Utzinger U (2012) Tryptophan fluorescence of cells and tissue in esophageal carcinoma. IEEE Sensors J 12:3273–3274
11. Li R, Dhankhar D, Chen J, Cesario TC, Rentzepis PM (2019) A tryptophan synchronous and normal fluorescence study on bacteria inactivation mechanism. Proc Natl Acad Sci 116: 18822–18826
12. Galas L, Gallavardin T, Bénard M, Lehner A, Schapman D, Lebon A, Komuro H, Lerouge P, Leleu S, Franck X (2018) "Probe, sample, and instrument (PSI)": the hat-trick for fluorescence live cell imaging. Chemosensors 6:40
13. Fu Y, Finney NS (2018) Small-molecule fluorescent probes and their design. RSC Adv 8: 29051–29061
14. Tian X, Murfin LC, Wu L, Lewis SE, James TD (2021) Fluorescent small organic probes for biosensing. Chem Sci 12:3406–3426
15. Huang Y, Zhang Y, Huo F, Wen Y, Yin C (2020) Design strategy and bioimaging of small organic molecule multicolor fluorescent probes. Sci China Chem 63(12):1742–1755
16. Chudakov DM, Matz MV, Lukyanov S, Lukyanov KA (2010) Fluorescent proteins and their applications in imaging living cells and tissues. Physiol Rev 90:1103–1163
17. Rodriguez EA, Campbell RE, Lin JY, Lin MZ, Miyawaki A, Palmer AE, Shu X, Zhang J, Tsien RY (2017) The growing and glowing toolbox of fluorescent and photoactive proteins. Trends Biochem Sci 42:111
18. Abbasi E, Kafshdooz T, Bakhtiary M, Nikzamir N, Nikzamir N, Nikzamir M, Mohammadian M, Akbarzadeh A (2016) Biomedical and biological applications of quantum dots. Artif Cells, Nanomed Biotechnol 44:885–891
19. Hatipoglu MK, Kelestemur S, Culha M (2016) Synthesis and biological applications of quantum dots. Springer, Cham, pp 505–534

20. Petryayeva E, Algar WR, Medintz IL (2013) Quantum dots in bioanalysis: a review of applications across various platforms for fluorescence spectroscopy and imaging. Appl Spectrosc 67:215–252
21. Zhou J, Yang Y, Zhang CY (2015) Toward biocompatible semiconductor quantum dots: from biosynthesis and bioconjugation to biomedical application. Chem Rev 115:11669–11717
22. Bilan R, Fleury F, Nabiev I, Sukhanova A (2015) Quantum dot surface chemistry and functionalization for cell targeting and imaging. Bioconjug Chem 26:609–624
23. Alivisatos AP, Gu W, Larabell C (2005) Quantum dots as cellular probes. Annu Rev Biomed Eng 7:55–76
24. Connell TU, James JL, White AR, Donnelly PS (2015) Protein labelling with versatile phosphorescent metal complexes for live cell luminescence imaging. Chem – A Eur J 21: 14146–14155
25. Fernández-Moreira V, Thorp-Greenwood FL, Coogan MP (2009) Application of d6 transition metal complexes in fluorescence cell imaging. Chem Commun 46:186–202
26. Tzubery A, Melamed-Book N, Tshuva EY (2018) Fluorescent antitumor titanium(IV) salen complexes for cell imaging. Dalton Trans 47:3669–3673
27. Cotruvo JA (2019) The chemistry of lanthanides in biology: recent discoveries, emerging principles, and technological applications. ACS Cent Sci 5:1496–1506
28. Cho U, Chen JK (2020) Lanthanide-based optical probes of biological systems. Cell Chem Biol 27:921–936
29. Mathieu E, Sipos A, Demeyere E, Phipps D, Sakaveli D, Borbas KE (2018) Lanthanide-based tools for the investigation of cellular environments. Chem Commun 54:10021–10035
30. Andraud C, Maury O (2009) Lanthanide complexes for nonlinear optics: from fundamental aspects to applications. Eur J Inorg Chem:4357–4371
31. Ge G, Li L, Wang D, Chen M, Zeng Z, Xiong W, Wu X, Guo C (2021) Carbon dots: synthesis, properties and biomedical applications. J Mater Chem B 9:6553–6575
32. Unnikrishnan B, Wu RS, Wei SC, Huang CC, Chang HT (2020) Fluorescent carbon dots for selective labeling of subcellular organelles. ACS Omega 5:11248–11261
33. Lesani P, Hazeera A, Hadi M, Lu Z, Palomba S, New EJ, Zreiqat H (2021) Design principles and biological applications of red-emissive two-photon carbon dots. Commun Mater 2(1): 1–12
34. Qu D, Wang X, Bao Y, Sun Z (2020) Recent advance of carbon dots in bio-related applications. J Phys Mater 3:022003
35. Jensen EC (2012) Use of fluorescent probes: their effect on cell biology and limitations. Anat Rec Adv Integr Anat Evol Biol 295:2031–2036
36. Wallace PK, Muirhead KA (2007) Cell tracking 2007: a proliferation of probes and applications. Immunol Investig 36:527–561
37. Chen M, He X, Wang K, He D, Yang X, Shi H (2014) Inorganic fluorescent nanoprobes for cellular and subcellular imaging. TrAC – Trends Anal Chem 58:120–129
38. Haque A, Faizi MSH, Rather JA, Khan MS (2017) Next generation NIR fluorophores for tumor imaging and fluorescence-guided surgery: a review. Bioorg Med Chem 25:2017–2034
39. Wan M, Zhu Y, Zou J (2020) Novel near-infrared fluorescent probe for live cell imaging. Exp Ther Med 19:1213
40. Tsubono Y, Kawamoto Y, Hidaka T, Pandian GN, Hashiya K, Bando T, Sugiyama H (2020) A near-infrared fluorogenic pyrrole-imidazole polyamide probe for live-cell imaging of telomeres. J Am Chem Soc 142:17356–17363
41. Liu X, Zhang QY, Wang F, Jiang JH (2019) A near infrared fluorescent probe for the detection and imaging of prolyl aminopeptidase activity in living cells. Analyst 144:5980–5985
42. Baeyer A (1871) Ueber eine neue Klasse von Farbstoffen. Ber Dtsch Chem Ges 4:555–558
43. Johnson I, Spence M (2010) Molecular probes handbook, a guide to fluorescent probes and labeling technologies.11th edn. Life Technologies, New York
44. Tsien RY, Waggoner A (1995) Fluorophores for confocal microscopy. In: Pawley JB (ed) Handbook of biological confocal microscopy. Springer, Boston, pp 267–279

45. Nanguneri S, Flottmann B, Herrmannsdörfer F, Kuner T, Heilemann M (2014) Single-molecule super-resolution imaging by tryptophan-quenching-induced photoswitching of phalloidin-fluorophore conjugates. Microsc Res Tech 77:510–516
46. Haenni D, Zosel F, Reymond L, Nettels D, Schuler B (2013) Intramolecular distances and dynamics from the combined photon statistics of single-molecule FRET and photoinduced electron transfer. J Phys Chem B 117:13015–13028
47. ISS 2021 lifetime data of selected fluorophores
48. Nakata E, Koshi Y, Koga E, Katayama Y, Hamachi I (2005) Double-modification of lectin using two distinct chemistries for fluorescent ratiometric sensing and imaging saccharides in test tube or in cell. J Am Chem Soc 127:13253–13261
49. Urban NT, Foreman MR, Hell SW, Sivan Y (2018) Nanoparticle-assisted STED nanoscopy with gold nanospheres. ACS Photonics 5:2574–2583
50. Adinolfi B, Pellegrino M, Tombelli S, Trono C, Giannetti A, Domenici C, Varchi G, Sotgiu G, Ballestri M, Baldini F (2018) Polymeric nanoparticles promote endocytosis of a survivin molecular beacon: localization and fate of nanoparticles and beacon in human A549 cells. Life Sci 215:106–112
51. Vogelsang J, Cordes T, Forthmann C, Steinhauer C, Tinnefeid P (2009) Controlling the fluorescence of ordinary oxazine dyes for single-molecule switching and superresolution microscopy. Proc Natl Acad Sci U S A 106:8107–8112
52. Ultzinger U (2011) Spectra database hosted at the University of Arizona
53. Kang HC, Haugland RP, Fisher PJ, Prendergast FG (1989) Spectral properties of 4-sulfonato-3,3′,5,5′-tetramethyl-2,2′-pyrronlethen-1,1′-borondifluoride complex (Bodipy), its sodium salt, and protein derivatives. In: Salzman GC (ed) New technologies in cytometry. SPIE, p 68
54. Moens PDJ, Bagatolli LA (2007) Profilin binding to sub-micellar concentrations of phosphatidylinositol (4,5) bisphosphate and phosphatidylinositol (3,4,5) trisphosphate. Biochim Biophys Acta 1768:439–449
55. Sauer M, Hofkens J, Enderlein J (2011) Fluorophores and fluorescent labels. In: Handbook of fluorescence spectroscopy and imaging. Wiley, Weinheim, pp 31–60
56. Texier I, Goutayer M, Da Silva A, Guyon L, Djaker N, Josserand V, Neumann E, Bibette J, Vinet F (2009) Cyanine-loaded lipid nanoparticles for improved in vivo fluorescence imaging. J Biomed Opt 14:054005
57. Lee IH, Saha S, Polley A, Huang H, Mayor S, Rao M, Groves JT (2015) Live cell plasma membranes do not exhibit a miscibility phase transition over a wide range of temperatures. J Phys Chem B 119:4450–4459
58. Georgiev R, Christova D, Todorova L, Georgieva B, Vasileva M, Novakov C, Babeva T (2018) Triblock copolymer micelles as templates for preparation of mesoporous niobia thin films. J Phys Conf Ser 992:012037
59. Gracetto AC, Batistela VR, Caetano W, De Oliveira HPM, Santos WG, Cavalheiro CCS, Hioka N (2010) Unusual 1,6-diphenyl-1,3,5-hexatriene (DPH) spectrophotometric behavior in water/ethanol and water/DMSO mixtures. J Braz Chem Soc 21:1497–1502
60. Hudson EN, Weber G (1973) Synthesis and characterization of two fluorescent sulfhydryl reagents. Biochemistry 12:4154–4161
61. Nunnally BK, He H, Li LC, Tucker SA, McGown LB (1997) Characterization of visible dyes for four-decay fluorescence detection in dna sequencing. Anal Chem 69:2392–2397
62. Strickler SJ, Berg RA (1962) Relationship between absorption intensity and fluorescence lifetime of molecules. J Chem Phys 37:814–822
63. Martin MM, Lindqvist L (1975) The pH dependence of fluorescein fluorescence. J Lumin 10: 381–390
64. Magde D, Rojas GE, Seybold PG (1999) Solvent dependence of the fluorescence lifetimes of xanthene dyes. Photochem Photobiol 70:737–744
65. Parasassi T, Gratton E (1995) Membrane lipid domains and dynamics as detected by Laurdan fluorescence. J Fluoresc 5:59–69

66. Fery-Forgues S, Fayet JP, Lopez A (1993) Drastic changes in the fluorescence properties of NBD probes with the polarity of the medium: involvement of a TICT state? J Photochem Photobiol A Chem 70:229–243
67. Lin S, Struve WS (1991) Time-resolved fluorescence of nitrobenzoxadiazole-aminohexanoic-acid: effect of intermolecular hydrogen-bonding on non-radiative decay. Photochem Photobiol 54:361–365
68. Amaro M, Filipe HAL, Prates Ramalho JP, Hof M, Loura LMS (2016) Fluorescence of nitrobenzoxadiazole (NBD)-labeled lipids in model membranes is connected not to lipid mobility but to probe location. Phys Chem Chem Phys 18:7042–7054
69. Tajalli H, Gilani AG, Zakerhamidi MS, Tajalli P (2008) The photophysical properties of Nile red and Nile blue in ordered anisotropic media. Dyes Pigments 78:15–24
70. Cser A, Nagy K, Biczók L (2002) Fluorescence lifetime of Nile Red as a probe for the hydrogen bonding strength with its microenvironment. Chem Phys Lett 360:473–478
71. Nimmerjahn A, Kirchhoff F, Kerr JND, Helmchen F (2004) Sulforhodamine 101 as a specific marker of astroglia in the neocortex in vivo. Nat Methods 1:31–37
72. Prendergast FG, Callahan PJ, Haugland RP (1981) 1-[4-(Trimethylamino)phenyl]-6-phenylhexa-1,3,5-triene: synthesis, fluorescence properties, and use as a fluorescence probe of lipid bilayers. Biochemistry 20:7333–7338
73. Kozma E, Kele P (2019) Fluorogenic probes for super-resolution microscopy. Org Biomol Chem 17:215–233
74. Wang L, Frei MS, Salim A, Johnsson K (2019) Small-molecule fluorescent probes for live-cell super-resolution microscopy. J Am Chem Soc 141:2770–2781
75. Lavis LD, Raines RT (2008) Bright ideas for chemical biology. ACS Chem Biol 3:142–155
76. Yang NJ, Hinner MJ (2015) Getting across the cell membrane: an overview for small molecules, peptides, and proteins. Methods Mol Biol 1266:29–53
77. Mobbs P, Becker D, Williamson R, Bate M, Warner A (1999) Techniques for dye injection and cell labelling. In: Microelectrode techniques. The Plymouth workshop handbook. The Company of Biologists Ltd, Cambridge, pp 361–387
78. Ji X, Ji K, Chittavong V, Aghoghovbia RE, Zhu M, Wang B (2017) Click and fluoresce: a bioorthogonally activated smart probe for wash-free fluorescent labeling of biomolecules. J Org Chem 82:1471–1476
79. Larsson A, Carlsson C, Jonsson M, Albinsson B (1994) Characterization of the binding of the fluorescent dyes YO and YOYO to DNA by polarized light spectroscopy. J Am Chem Soc 116:8459–8465
80. Hirons GT, Fawcett JJ, Crissman HA (1994) TOTO and YOYO: new very bright fluorochromes for DNA content analyses by flow cytometry. Cytometry 15:129–140
81. Lichtman JW, Conchello JA (2005) Fluorescence microscopy. Nat Methods 2:910–919
82. Vira S, Mekhedov E, Humphrey G, Blank PS (2010) Fluorescent-labeled antibodies: balancing functionality and degree of labeling. Anal Biochem 402:146–150
83. Szabó Á, Szendi-Szatmári T, Ujlaky-Nagy L, Rádi I, Vereb G, Szöllősi J, Nagy P (2018) The effect of fluorophore conjugation on antibody affinity and the photophysical properties of dyes. Biophys J 114:688–700
84. Cosa G, Focsaneanu K-S, McLean JRN, McNamee JP, Scaiano JC (2001) Photophysical properties of fluorescent DNA-dyes bound to single- and double-stranded DNA in aqueous buffered solution. Photochem Photobiol 73:585
85. Mullins JM (2010) Fluorochromes: properties and characteristics. Methods Mol Biol 588: 123–134
86. Li Q, Seeger S (2011) Multidonor deep-UV FRET study of protein – ligand binding and its potential to obtain structure information. J Phys Chem B 115:13643–13649
87. Berlman I (1971) Handbook of fluorescence spectra of aromatic molecules.2nd edn. Elsevier
88. Chen H, Ahsan SS, Santiago-Berrios MB, Abruña HD, Webb WW (2010) Mechanisms of quenching of alexa fluorophores by natural amino acids. J Am Chem Soc 132:7244–7245

89. Marmé N, Knemeyer JP, Sauer M, Wolfrum J (2003) Inter- and intramolecular fluorescence quenching of organic dyes by tryptophan. Bioconjug Chem 14:1133–1139
90. Neuweiler H, Schulz A, Vaiana AC, Smith JC, Kaul S, Wolfrum J, Sauer M (2002) Detection of individual p53-autoantibodies by using quenched peptide-based molecular probes. Angew Chem Int Ed 41:4769–4773
91. Eggeling C, Widengren J, Rigler R, Seidel CAM (1998) Photobleaching of fluorescent dyes under conditions used for single-molecule detection: evidence of two-step photolysis. Anal Chem 70:2651–2659
92. Diaspro A, Chirico G, Usai C, Ramoino P, Dobrucki J (2006) Photobleaching. In: Handbook of biological confocal microscopy. Springer, Boston, pp 690–702
93. Vogelsang J, Kasper R, Steinhauer C, Person B, Heilemann M, Sauer M, Tinnefeld P (2008) A reducing and oxidizing system minimizes photobleaching and blinking of fluorescent dyes. Angew Chem Int Ed 47:5465–5469
94. Demchenko AP (2020) Photobleaching of organic fluorophores: quantitative characterization, mechanisms, protection. Methods Appl Fluoresc 8:022001
95. Panchuk-Voloshina N, Haugland RP, Bishop-Stewart J, Bhalgat MK, Millard PJ, Mao F, Leung WY, Haugland RP (1999) Alexa dyes, a series of new fluorescent dyes that yield exceptionally bright, photostable conjugates. J Histochem Cytochem 47:1179–1188
96. Mitronova GY, Belov VN, Bossi ML, Wurm CA, Meyer L, Medda R, Moneron G, Bretschneider S, Eggeling C, Jakobs S, Hell SW (2010) New fluorinated rhodamines for optical microscopy and nanoscopy. Chem – A Eur J 16:4477–4488
97. Heilemann M, Van De Linde S, Mukherjee A, Sauer M (2009) Super-resolution imaging with small organic fluorophores. Angew Chem Int Ed 48:6903–6908
98. Hnedzko D, McGee DW, Rozners E (2016) Synthesis and properties of peptide nucleic acid labeled at the N-terminus with HiLyte Fluor 488 fluorescent dye. Bioorg Med Chem 24:4199–4205
99. Grimm JB, English BP, Chen J, Slaughter JP, Zhang Z, Revyakin A, Patel R, Macklin JJ, Normanno D, Singer RH, Lionnet T, Lavis LD (2015) A general method to improve fluorophores for live-cell and single-molecule microscopy. Nat Methods 12:244–250
100. Hinkeldey B, Schmitt A, Jung G (2008) Comparative photostability studies of BODIPY and fluorescein dyes by using fluorescence correlation spectroscopy. ChemPhysChem 9:2019–2027
101. Gorka AP, Schnermann MJ (2016) Harnessing cyanine photooxidation: from slowing photobleaching to near-IR uncaging. Curr Opin Chem Biol 33:117–125
102. Zheng Q, Jockusch S, Zhou Z, Blanchard SC (2014) The contribution of reactive oxygen species to the photobleaching of organic fluorophores. Photochem Photobiol 90:448–454
103. Yguerabide J, Schmidt JA, Yguerabide EE (1982) Lateral mobility in membranes as detected by fluorescence recovery after photobleaching. Biophys J 40:69–75
104. Ishikawa-Ankerhold HC, Ankerhold R, Drummen GPC (2012) Advanced fluorescence microscopy techniques–FRAP, FLIP, FLAP, FRET and FLIM. Molecules 17:4047–4132
105. Gruber HJ, Hahn CD, Kada G, Riener CK, Harms GS, Ahrer W, Dax TG, Knaus HG (2000) Anomalous fluorescence enhancement of Cy3 and Cy3.5 versus anomalous fluorescence loss of Cy5 and Cy7 upon covalent linking to IgG and noncovalent binding to avidin. Bioconjug Chem 11:696–704
106. Gebhardt C, Lehmann M, Reif MM, Zacharias M, Gemmecker G, Cordes T (2021) Molecular and spectroscopic characterization of green and red cyanine fluorophores from the Alexa Fluor and AF series. ChemPhysChem 22:1566–1583
107. Valdes-Aguilera O, Neckers DC (1989) Aggregation phenomena in xanthene dyes. Acc Chem Res 22:171–177
108. Demchenko AP (2009) Introduction to fluorescence sensing. Springer, Dordrecht
109. Bergström F, Mikhalyov I, Hägglöf P, Wortmann R, Ny T, Johansson LBÅ (2002) Dimers of dipyrrometheneboron difluoride (BODIPY) with light spectroscopic applications in chemistry and biology. J Am Chem Soc 124:196–204

110. Monteiro ME, Sarmento MJ, Fernandes F (2014) Role of calcium in membrane interactions by PI(4,5)P2 – binding proteins. Biochem Soc Trans 42:1441–1446
111. Dziuba D, Jurkiewicz P, Cebecauer M, Hof M, Hocek M (2016) A rotational BODIPY nucleotide: an environment-sensitive fluorescence-lifetime probe for DNA interactions and applications in live-cell microscopy. Angew Chem 128:182–186
112. Song X, Li N, Wang C, Xiao Y (2017) Targetable and fixable rotor for quantifying mitochondrial viscosity of living cells by fluorescence lifetime imaging. J Mater Chem B 5:360–368
113. Leung RWK, Yeh S-CA, Fang Q (2011) Effects of incomplete decay in fluorescence lifetime estimation. Biomed Opt Express 2:2517–2531
114. Lavis LD, Rutkoski TJ, Raines RT (2007) Tuning the pK a of fluorescein to optimize binding assays environment. The fluorescence of the dye varies likewise. Life Sci 79:6775–6782
115. Haugland RP (2005) The molecular probes handbook: a guide to fluorescent probes and labeling technologies. Invitrogen Corp, Karlsbad
116. Paradiso AM, Tsien RY, Machen TE (1984) Na+-H+ exchange in gastric glands as measured with a cytoplasmic-trapped, fluorescent pH indicator. Proc Natl Acad Sci 81:7436–7440
117. Rink TI, Tsien RY, Pozzan T (1982) Cytoplasmic pH and free Mg2+ in lymphocytes. J Cell Biol 95:189–196
118. Yoshihara T, Maruyama R, Shiozaki S, Yamamoto K, Kato SI, Nakamura Y, Tobita S (2020) Visualization of lipid droplets in living cells and fatty livers of mice based on the fluorescence of π-extended coumarin using fluorescence lifetime imaging microscopy. Anal Chem 92: 4996–5003
119. Yang D, Dai SY (2020) A visible and near-infrared light activatable diazocoumarin probe for fluorogenic protein labeling in living cells. J Am Chem Soc 142:17156–17166
120. Sun W, Guo S, Hu C, Fan J, Peng X (2016) Recent development of chemosensors based on cyanine platforms. Chem Rev 116:7768–7817
121. Shindy HA (2017) Fundamentals in the chemistry of cyanine dyes: a review. Dyes Pigments 145:505–513
122. Zheng Q, Lavis LD (2017) Development of photostable fluorophores for molecular imaging. Curr Opin Chem Biol 39:32–38
123. Li G, Guan Y, Ye F, Liu SH, Yin J (2020) Cyanine-based fluorescent indicator for mercury ion and bioimaging application in living cells. Spectrochim Acta A Mol Biomol Spectrosc 239: 118465
124. Uno K, Sugimoto N, Sato Y (2021) N-aryl pyrido cyanine derivatives are nuclear and organelle DNA markers for two-photon and super-resolution imaging. Nat Commun 12(1): 1–9
125. Aristova D, Kosach V, Chernii S, Slominsky Y, Balanda A, Filonenko V, Yarmoluk S, Rotaru A, Özkan HG, Mokhir A, Kovalska V (2021) Monomethine cyanine probes for visualization of cellular RNA by fluorescence microscopy. Methods Appl Fluoresc 9:045002
126. Beija M, Afonso CAM, Martinho JMG (2009) Synthesis and applications of rhodamine derivatives as fluorescent probes. Chem Soc Rev 38:2410–2433
127. Duan Y, Liu M, Sun W, Wang M, Liu S, Li Q (2009) Recent progress on synthesis of fluorescein probes. Mini Rev Org Chem 6:35–43
128. Rajasekar M (2021) Recent development in fluorescein derivatives. J Mol Struct 1224:129085
129. Le Guern F, Mussard V, Gaucher A, Rottman M, Prim D (2020) Fluorescein derivatives as fluorescent probes for ph monitoring along recent biological applications. Int J Mol Sci 21: 1–23
130. Loudet A, Burgess K (2007) BODIPY dyes and their derivatives: syntheses and spectroscopic properties. Chem Rev 107:4891–4932
131. Martynov VI, Pakhomov AA (2021) BODIPY derivatives as fluorescent reporters of molecular activities in living cells. Russ Chem Rev 90:1213–1262
132. Yue J, Tao Y, Zhang J, Wang H, Wang N, Zhao W (2021) BODIPY-based fluorescent probe for fast detection of hydrogen sulfide and lysosome-targeting applications in living cells. Chem – An Asian J 16:850–855

133. Toseland CP (2013) Fluorescent labeling and modification of proteins. J Chem Biol 6:85–95
134. Obermaier C, Griebel A, Westermeier R (2015) Principles of protein labeling techniques. Methods Mol Biol 1295:153–165
135. Sereda TJ, Mant CT, Quinn AM, Hodges RS (1993) Effect of the alpha-amino group on peptide retention behaviour in reversed-phase chromatography. Determination of the pK (a) values of the alpha-amino group of 19 different N-terminal amino acid residues. J Chromatogr 646:17–30
136. Giepmans BNG, Adams SR, Ellisman MH, Tsien RY (2006) The fluorescent toolbox for assessing protein location and function. Science 312:217–224
137. Fernández-Suárez M, Ting AY (2008) Fluorescent probes for super-resolution imaging in living cells. Nat Rev Mol Cell Biol 9:929–943
138. Klein A, Hank S, Raulf A, Joest EF, Tissen F, Heilemann M, Wieneke R, Tampé R (2018) Live-cell labeling of endogenous proteins with nanometer precision by transduced nanobodies. Chem Sci 9:7835
139. Herce HD, Schumacher D, Schneider AFL, Ludwig AK, Mann FA, Fillies M, Kasper MA, Reinke S, Krause E, Leonhardt H, Cardoso MC, Hackenberger CPR (2017) Cell-permeable nanobodies for targeted immunolabelling and antigen manipulation in living cells. Nat Chem 9(8):762–771
140. Traenkle B, Rothbauer U (2017) Under the microscope: single-domain antibodies for live-cell imaging and super-resolution microscopy. Front Immunol 8:1030
141. Hoelzel CA, Zhang X (2020) Visualizing and manipulating biological processes by using HaloTag and SNAP-tag technologies. ChemBioChem 21:1935–1946
142. Los GV, Encell LP, McDougall MG, Hartzell DD, Karassina N, Zimprich C, Wood MG, Learish R, Ohana RF, Urh M, Simpson D, Mendez J, Zimmerman K, Otto P, Vidugiris G, Zhu J, Darzins A, Klaubert DH, Bulleit RF, Wood KV (2008) HaloTag: a novel protein labeling technology for cell imaging and protein analysis. ACS Chem Biol 3:373–382
143. Keppler A, Gendreizig S, Gronemeyer T, Pick H, Vogel H, Johnsson K (2002) A general method for the covalent labeling of fusion proteins with small molecules in vivo. Nat Biotechnol 21(1):86–89
144. Juillerat A, Gronemeyer T, Keppler A, Gendreizig S, Pick H, Vogel H, Johnsson K (2003) Directed evolution of O6-alkylguanine-DNA alkyltransferase for efficient labeling of fusion proteins with small molecules in vivo. Chem Biol 10:313–317
145. Gautier A, Juillerat A, Heinis C, Corrêa IR, Kindermann M, Beaufils F, Johnsson K (2008) An engineered protein tag for multiprotein labeling in living cells. Chem Biol 15:128–136
146. Miller LW, Cai Y, Sheetz MP, Cornish VW (2005) In vivo protein labeling with trimethoprim conjugates: a flexible chemical tag. Nat Methods 2:255–257
147. Mizukami S, Watanabe S, Hori Y, Kikuchi K (2009) Covalent protein labeling based on noncatalytic β-lactamase and a designed FRET substrate. J Am Chem Soc 131:5016–5017
148. Hori Y, Ueno H, Mizukami S, Kikuchi K (2009) Photoactive yellow protein-based protein labeling system with turn-on fluorescence intensity. J Am Chem Soc 131:16610–16611
149. Liu Y, Zhang X, Tan YL, Bhabha G, Ekiert DC, Kipnis Y, Bjelic S, Baker D, Kelly JW (2014) De novo-designed enzymes as small-molecule-regulated fluorescence imaging tags and fluorescent reporters. J Am Chem Soc 136:13102–13105
150. Liu Y, Miao K, Li Y, Fares M, Chen S, Zhang X (2018) A HaloTag-based multicolor fluorogenic sensor visualizes and quantifies proteome stress in live cells using solvatochromic and molecular rotor-based fluorophores. Biochemistry 57:4663–4674
151. Adams SR (2008) Tags and probes for chemical biology: the biarsenical-tetracysteine protein tag: chemistry and biological applications. In: Chemical biology: from small molecules to systems biology and drug design, vol 1–3. Wiley, pp 427–457
152. Sarmento MJ, Oneto M, Pelicci S, Pesce L, Scipioni L, Faretta M, Furia L, Dellino GI, Pelicci PG, Bianchini P, Diaspro A, Lanzanò L (2018) Exploiting the tunability of stimulated emission depletion microscopy for super-resolution imaging of nuclear structures. Nat Commun 9:3415

153. Liang L, Astruc D (2011) The copper(I)-catalyzed alkyne-azide cycloaddition (CuAAC) "click" reaction and its applications. An overview. Coord Chem Rev 255:2933–2945
154. Presolski SI, Hong VP, Finn MG (2011) Copper-catalyzed azide–alkyne click chemistry for bioconjugation. Curr Protoc Chem Biol 3:153–162
155. Gutmann M, Memmel E, Braun AC, Seibel J, Meinel L, Lühmann T (2016) Biocompatible azide-alkyne "click" reactions for surface decoration of glyco-engineered cells. ChemBioChem 17:866–875
156. Baskin JM, Prescher JA, Laughlin ST, Agard NJ, Chang PV, Miller IA, Lo A, Codelli JA, Bertozzi CR (2007) Copper-free click chemistry for dynamic in vivo imaging. Proc Natl Acad Sci 104:16793–16797
157. Saxon E, Bertozzi CR (2000) Cell surface engineering by a modified Staudinger reaction. Science 287:2007–2010
158. Li L, Zhang Z (2016) Development and applications of the copper-catalyzed azide-alkyne cycloaddition (CuAAC) as a bioorthogonal reaction. Molecules 21:1393
159. Laxman P, Ansari S, Gaus K, Goyette J (2021) The benefits of unnatural amino acid incorporation as protein labels for single molecule localization microscopy. Front Chem 9:161
160. Lee KJ, Kang D, Park HS (2019) Site-specific labeling of proteins using unnatural amino acids. Mol Cells 42:386–396
161. Saal KA, Richter F, Rehling P, Rizzoli SO (2018) Combined use of unnatural amino acids enables dual-color super-resolution imaging of proteins via cick chemistry. ACS Nano 12: 12247–12254
162. Brown W, Liu J, Deiters A (2018) Genetic code expansion in animals. ACS Chem Biol 13: 2375–2386
163. Wiltschi B (2016) Incorporation of non-canonical amino acids into proteins in yeast. Fungal Genet Biol 89:137–156
164. Ambrogelly A, Palioura S, Söll D (2007) Natural expansion of the genetic code. Nat Chem Biol 3(1):29–35
165. Jakob L, Gust A, Grohmann D (2019) Evaluation and optimisation of unnatural amino acid incorporation and bioorthogonal bioconjugation for site-specific fluorescent labelling of proteins expressed in mammalian cells. Biochem Biophys Rep 17:1–9
166. Lang K, Chin JW (2014) Cellular incorporation of unnatural amino acids and bioorthogonal labeling of proteins. Chem Rev 114:4764–4806
167. Chin JW (2014) Expanding and reprogramming the genetic code of cells and animals. Annu Rev Biochem 83:379–408
168. Chazotte B (2011) Labeling membrane glycoproteins or glycolipids with fluorescent wheat germ agglutinin. Cold Spring Harb Protoc:6
169. Honig MG, Hume RI (1986) Fluorescent carbocyanine dyes allow living neurons of identified origin to be studied in long-term cultures. J Cell Biol 103:171–187
170. Kleusch C, Hersch N, Hoffmann B, Merkel R, Csiszár A (2012) Fluorescent lipids: functional parts of fusogenic liposomes and tools for cell membrane labeling and visualization. Molecules 17:1055–1073
171. Bolte S, Talbot C, Boutte Y, Catrice O, Read ND, Satiat-Jeunemaitre B (2004) FM-dyes as experimental probes for dissecting vesicle trafficking in living plant cells. J Microsc 214:159–173
172. Betz WJ, Bewick GS (1993) Optical monitoring of transmitter release and synaptic vesicle recycling at the frog neuromuscular junction. J Physiol 460:287–309
173. Sýkora J, Kapusta P, Fidler V, Hof M (2002) On what time scale does solvent relaxation in phospholipid bilayers happen? Langmuir 18:571–574
174. Loura LMS, Prates Ramalho JP (2009) Fluorescent membrane probes' behavior in lipid bilayers: insights from molecular dynamics simulations. Biophys Rev 1:141–148
175. Lee AG (2004) How lipids affect the activities of integral membrane proteins. Biochim Biophys Acta 1666:62–87

176. Reits EAJ, Neefjes JJ (2001) From fixed to FRAP: measuring protein mobility and activity in living cells. Nat Cell Biol 3:E145
177. Macháň R, Hof M (2010) Lipid diffusion in planar membranes investigated by fluorescence correlation spectroscopy. Biochim Biophys Acta Biomembr 1798:1377–1391
178. do Canto AMTM, Robalo JR, Santos PD, Carvalho AJP, Ramalho JPP, Loura LMS (2016) Diphenylhexatriene membrane probes DPH and TMA-DPH: a comparative molecular dynamics simulation study. Biochim Biophys Acta Biomembr 1858:2647–2661
179. Lentz BR (1989) Membrane "fluidity" as detected by diphenylhexatriene probes. Chem Phys Lipids 50:171–190
180. Lentz BR (1993) Use of fluorescent probes to monitor molecular order and motions within liposome bilayers. Chem Phys Lipids 64:99–116
181. Sklar LA, Hudson BS, Simoni RD (1977) Conjugated polyene fatty acids as fluorescent probes: synthetic phospholipid membrane studies. Biochemistry 16:819–828
182. Nyholm TKM, Lindroos D, Westerlund B, Slotte JP (2011) Construction of a DOPC/PSM/cholesterol phase diagram based on the fluorescence properties of trans-parinaric acid. Langmuir 27:8339–8350
183. de Almeida RFM, Fedorov A, Prieto M (2003) Sphingomyelin/phosphatidylcholine/cholesterol phase diagram: boundaries and composition of lipid rafts. Biophys J 85:2406–2416
184. Haidekker MA, Theodorakis EA (2007) Molecular rotors – fluorescent biosensors for viscosity and flow. Org Biomol Chem 5:1669–1678
185. Kuimova MK (2012) Mapping viscosity in cells using molecular rotors. Phys Chem Chem Phys 14:12671–12686
186. Amaro M, Reina F, Hof M, Eggeling C, Sezgin E (2017) Laurdan and Di-4-ANEPPDHQ probe different properties of the membrane. J Phys D Appl Phys 50:134004
187. Shimomura O, Johnson FH, Saiga Y (1962) Extraction, purification and properties of aequorin, a bioluminescent protein from the luminous hydromedusan, Aequorea. J Cell Comp Physiol 59:223–239
188. Heim R, Prasher DC, Tsien RY (1994) Wavelength mutations and posttranslational autoxidation of green fluorescent protein. Proc Natl Acad Sci U S A 91:12501
189. Subach OM, Gundorov IS, Yoshimura M, Subach FV, Zhang J, Grüenwald D, Souslova EA, Chudakov DM, Verkhusha VV (2008) Conversion of red fluorescent protein into a bright blue probe. Chem Biol 15:1116–1124
190. Goedhart J, Von Stetten D, Noirclerc-Savoye M, Lelimousin M, Joosen L, Hink MA, Van Weeren L, Gadella TWJ, Royant A (2012) Structure-guided evolution of cyan fluorescent proteins towards a quantum yield of 93%. Nat Commun 3:751
191. Markwardt ML, Kremers G-J, Kraft CA, Ray K, Cranfill PJC, Wilson KA, Day RN, Wachter RM, Davidson MW, Rizzo MA (2011) An improved cerulean fluorescent protein with enhanced brightness and reduced reversible photoswitching. PLoS One 6:e17896
192. Cormack BP, Valdivia RH, Falkow S (1996) FACS-optimized mutants of the green fluorescent protein (GFP). Gene 173:33–38
193. Grotjohann T, Testa I, Leutenegger M, Bock H, Urban NT, Lavoie-Cardinal F, Willig KI, Eggeling C, Jakobs S, Hell SW (2011) Diffraction-unlimited all-optical imaging and writing with a photochromic GFP. Nature 478:204–208
194. Zhang X, Zhang M, Li D, He W, Peng J, Betzig E, Xu P (2016) Highly photostable, reversibly photoswitchable fluorescent protein with high contrast ratio for live-cell superresolution microscopy. Proc Natl Acad Sci U S A 113:10364–10369
195. Zapata-Hommer O, Griesbeck O (2003) Efficiently folding and circularly permuted variants of the sapphire mutant of GFP. BMC Biotechnol 3:5
196. Campbell BC, Nabel EM, Murdock MH, Lao-Peregrin C, Tsoulfas P, Blackmore MG, Lee FS, Liston C, Morishita H, Petsko GA (2020) mGreenLantern: a bright monomeric fluorescent protein with rapid expression and cell filling properties for neuronal imaging. Proc Natl Acad Sci U S A 117:30710–30721

197. Shaner NC, Lambert GG, Chammas A, Ni Y, Cranfill PJ, Baird MA, Sell BR, Allen JR, Day RN, Israelsson M, Davidson MW, Wang J (2013) A bright monomeric green fluorescent protein derived from Branchiostoma lanceolatum. Nat Methods 10:407–409
198. Patterson GH, Lippincott-Schwartz J (2002) A photoactivatable GFP for selective photolabeling of proteins and cells. Science 297:1873–1877
199. Bajar BT, Wang ES, Lam AJ, Kim BB, Jacobs CL, Howe ES, Davidson MW, Lin MZ, Chu J (2016) Improving brightness and photostability of green and red fluorescent proteins for live cell imaging and FRET reporting. Sci Rep 6:1–12
200. Stiel AC, Trowitzsch S, Weber G, Andresen M, Eggeling C, Hell SW, Jakobs S, Wahl MC (2007) 1.8 Å bright-state structure of the reversibly switchable fluorescent protein Dronpa guides the generation of fast switching variants. Biochem J 402:35–42
201. Ai HW, Hazelwood KL, Davidson MW, Campbell RE (2008) Fluorescent protein FRET pairs for ratiometric imaging of dual biosensors. Nat Methods 5:401–403
202. Ormö M, Cubitt AB, Kallio K, Gross LA, Tsien RY, Remington SJ (1996) Crystal structure of the Aequorea victoria green fluorescent protein. Science 273:1392–1395
203. Kremers GJ, Goedhart J, Van Munster EB, Gadella TWJ (2006) Cyan and yellow super fluorescent proteins with improved brightness, protein folding, and FRET förster radius. Biochemistry 45:6570–6580
204. Zacharias DA, Violin JD, Newton AC, Tsien RY (2002) Partitioning of lipid-modified monomeric GFPs into membrane microdomains of live cells. Science 296:913–916
205. Shaner NC, Campbell RE, Steinbach PA, Giepmans BNG, Palmer AE, Tsien RY (2004) Improved monomeric red, orange and yellow fluorescent proteins derived from Discosoma sp. red fluorescent protein. Nat Biotechnol 22:1567–1572
206. Matz MV, Fradkov AF, Labas YA, Savitsky AP, Zaraisky AG, Markelov ML, Lukyanov SA (1999) Fluorescent proteins from nonbioluminescent Anthozoa species. Nat Biotechnol 17: 969–973
207. Pletnev S, Subach FV, Dauter Z, Wlodawer A, Verkhusha VV (2012) A structural basis for reversible photoswitching of absorbance spectra in red fluorescent protein rsTagRFP. J Mol Biol 417:144–151
208. Shaner NC, Lin MZ, McKeown MR, Steinbach PA, Hazelwood KL, Davidson MW, Tsien RY (2008) Improving the photostability of bright monomeric orange and red fluorescent proteins. Nat Methods 5:545–551
209. Bindels DS, Haarbosch L, Van Weeren L, Postma M, Wiese KE, Mastop M, Aumonier S, Gotthard G, Royant A, Hink MA, Gadella TWJ (2016) MScarlet: a bright monomeric red fluorescent protein for cellular imaging. Nat Methods 14:53–56
210. Subach FV, Patterson GH, Manley S, Gillette JM, Lippincott-Schwartz J, Verkhusha VV (2009) Photoactivatable mCherry for high-resolution two-color fluorescence microscopy. Nat Methods 6:153–159
211. Subach FV, Patterson GH, Renz M, Lippincott-Schwartz J, Verkhusha VV (2010) Bright monomeric photoactivatable red fluorescent protein for two-color super-resolution sptPALM of live cells. J Am Chem Soc 132:6481–6491
212. Kogure T, Karasawa S, Araki T, Saito K, Kinjo M, Miyawaki A (2006) A fluorescent variant of a protein from the stony coral Montipora facilitates dual-color single-laser fluorescence cross-correlation spectroscopy. Nat Biotechnol 24:577–581
213. Gunewardene MS, Subach FV, Gould TJ, Penoncello GP, Gudheti MV, Verkhusha VV, Hess ST (2011) Superresolution imaging of multiple fluorescent proteins with highly overlapping emission spectra in living cells. Biophys J 101:1522–1528
214. Shcherbo D, Murphy CS, Ermakova GV, Solovieva EA, Chepurnykh TV, Shcheglov AS, Verkhusha VV, Pletnev VZ, Hazelwood KL, Roche PM, Lukyanov S, Zaraisky AG, Davidson MW, Chudakov DM (2009) Far-red fluorescent tags for protein imaging in living tissues. Biochem J 418:567–574
215. Lin MZ, McKeown MR, Ng HL, Aguilera TA, Shaner NC, Campbell RE, Adams SR, Gross LA, Ma W, Alber T, Tsien RY (2009) Autofluorescent proteins with excitation in the optical window for intravital imaging in mammals. Chem Biol 16:1169–1179

216. Shagin DA, Barsova EV, Yanushevich YG, Fradkov AF, Lukyanov KA, Labas YA, Semenova TN, Ugalde JA, Meyers A, Nunez JM, Widder EA, Lukyanov SA, Matz MV (2004) GFP-like proteins as ubiquitous metazoan superfamily: evolution of functional features and structural complexity. Mol Biol Evol 21:841–850
217. Deheyn DD, Kubokawa K, Mccarthy JK, Murakami A, Porrachia M, Rouse GW, Holland ND (2007) Endogenous green fluorescent protein (GFP) in amphioxus. Biol Bull 213:95–100
218. Jradi FM, Lavis LD (2019) Chemistry of photosensitive fuorophores for single-molecule localization microscopy. ACS Chem Biol 14:1077–1090
219. Santos EM, Sheng W, Esmatpour Salmani R, Tahmasebi Nick S, Ghanbarpour A, Gholami H, Vasileiou C, Geiger JH, Borhan B (2021) Design of large Stokes shift fluorescent proteins based on excited state proton transfer of an engineered photobase. J Am Chem Soc 143: 15091–15102
220. Zhao B, Ding W, Tan Z, Tang Q, Zhao K (2019) A large stokes shift fluorescent protein constructed from the fusion of red fluorescent mCherry and far-red fuorescent BDFP1.6. ChemBioChem 20:1167–1173
221. Piatkevich KD, Hulit J, Subach OM, Wu B, Abdulla A, Segall JE, Verkhusha VV (2010) Monomeric red fluorescent proteins with a large Stokes shift. Proc Natl Acad Sci 107:5369–5374
222. Piatkevich KD, Malashkevich VN, Morozova KS, Nemkovich NA, Almo SC, Verkhusha VV (2013) Extended stokes shift in fluorescent proteins: chromophore-protein interactions in a near-infrared TagRFP675 variant. Sci Rep 3:1–11
223. Khmelinskii A, Keller PJ, Bartosik A, Meurer M, Barry JD, Mardin BR, Kaufmann A, Trautmann S, Wachsmuth M, Pereira G, Huber W, Schiebel E, Knop M (2012) Tandem fluorescent protein timers for in vivo analysis of protein dynamics. Nat Biotechnol 30(7): 708–714
224. Shcherbo D, Merzlyak EM, Chepurnykh TV, Fradkov AF, Ermakova GV, Solovieva EA, Lukyanov KA, Bogdanova EA, Zaraisky AG, Lukyanov S, Chudakov DM (2007) Bright far-red fluorescent protein for whole-body imaging. Nat Methods 4:741–746
225. Baird GS, Zacharias DA, Tsien RY (2000) Biochemistry, mutagenesis, and oligomerization of DsRed, a red fluorescent protein from coral. Proc Natl Acad Sci 97:11984–11989
226. Zhang J, Campbell RE, Ting AY, Tsien RY (2002) Creating new fluorescent probes for cell biology. Nat Rev Mol Cell Biol 3:906–918
227. Zacharias DA (2002) Sticky caveats in an otherwise glowing report: oligomerizing fluorescent proteins and their use in cell biology. Sci STKE 2002(131):pe23
228. Tsien RY (1999) Rosy dawn for fluorescent proteins. Nat Biotechnol 17(10):956–957
229. Mishin AS, Belousov VV, Solntsev KM, Lukyanov KA (2015) Novel uses of fluorescent proteins. Curr Opin Chem Biol 27:1–9
230. Stepanenko OV, Stepanenko OV, Shcherbakova DM, Kuznetsova IM, Turoverov KK, Verkhusha VV (2011) Modern fluorescent proteins: from chromophore formation to novel intracellular applications. BioTechniques 51:313–327
231. Davidson MW, Campbell RE (2009) Engineered fluorescent proteins: innovations and applications. Nat Methods 6(10):713–717
232. Kim H, Ju J, Lee HN, Chun H, Seong J (2021) Genetically encoded biosensors based on fluorescent proteins. Sensors (Switzerland) 21:1–18
233. Burgstaller S, Bischof H, Gensch T, Stryeck S, Gottschalk B, Ramadani-Muja J, Eroglu E, Rost R, Balfanz S, Baumann A, Waldeck-Weiermair M, Hay JC, Madl T, Graier WF, Malli R (2019) PH-lemon, a fluorescent protein-based pH reporter for acidic compartments. ACS Sensors 4:883–891
234. Tutol JN, Peng W, Dodani SC (2019) Discovery and characterization of a naturally occurring, turn-on yellow fluorescent protein sensor for chloride. Biochemistry 58:31–35
235. Yu X, Strub MP, Barnard TJ, Noinaj N, Piszczek G, Buchanan SK, Taraska JW (2014) An engineered palette of metal ion quenchable fluorescent proteins. PLoS One 9:e95808

236. Hanson GT, Aggeler R, Oglesbee D, Cannon M, Capaldi RA, Tsien RY, Remington SJ (2004) Investigating mitochondrial redox potential with redox-sensitive green fluorescent protein indicators. J Biol Chem 279:13044–13053
237. Pak VV, Ezeriņa D, Lyublinskaya OG, Pedre B, Tyurin-Kuzmin PA, Mishina NM, Thauvin M, Young D, Wahni K, Martínez Gache SA, Demidovich AD, Ermakova YG, Maslova YD, Shokhina AG, Eroglu E, Bilan DS, Bogeski I, Michel T, Vriz S, Messens J, Belousov VV (2020) Ultrasensitive genetically encoded indicator for hydrogen peroxide identifies roles for the oxidant in cell migration and mitochondrial function. Cell Metab 31: 642–653.e6
238. Baker BJ, Mutoh H, Dimitrov D, Akemann W, Perron A, Iwamoto Y, Jin L, Cohen LB, Isacoff EY, Pieribone VA, Hughes T, Knöpfel T (2008) Genetically encoded fluorescent sensors of membrane potential. Brain Cell Biol 36:53–67
239. Hochreiter B, Garcia AP, Schmid JA (2015) Fluorescent proteins as genetically encoded FRET biosensors in life sciences. Sensors (Basel) 15:26281–26314
240. Miyawaki A, Llopis J, Heim R, Michael McCaffery J, Adams JA, Ikura M, Tsien RY (1997) Fluorescent indicators for Ca2+ based on green fluorescent proteins and calmodulin. Nature 388:882–887
241. Calamera G, Li D, Ulsund AH, Kim JJ, Neely OC, Moltzau LR, Bjørnerem M, Paterson D, Kim C, Levy FO, Andressen KW (2019) FRET-based cyclic GMP biosensors measure low cGMP concentrations in cardiomyocytes and neurons. Commun Biol 2(1):1–12
242. Maryu G, Matsuda M, Aoki K (2016) Multiplexed fluorescence imaging of ERK and akt activities and cell-cycle progression. Cell Struct Funct 41:81–92
243. Cranfill PJ, Sell BR, Baird MA, Allen JR, Lavagnino Z, De Gruiter HM, Kremers GJ, Davidson MW, Ustione A, Piston DW (2016) Quantitative assessment of fluorescent proteins. Nat Methods 13(7):557–562
244. Kremers GJ, Gilbert SG, Cranfill PJ, Davidson MW, Piston DW (2011) Fluorescent proteins at a glance. J Cell Sci 124:157–160
245. Kaishima M, Ishii J, Matsuno T, Fukuda N, Kondo A (2016) Expression of varied GFPs in Saccharomyces cerevisiae: codon optimization yields stronger than expected expression and fluorescence intensity. Sci Rep 6(1):1–15
246. Van Genechten W, Demuyser L, Dedecker P, Van Dijck P (2020) Presenting a codon-optimized palette of fluorescent proteins for use in Candida albicans. Sci Rep 10:1–9
247. Chen X, Zaro JL, Shen WC (2013) Fusion protein linkers: property, design and functionality. Adv Drug Deliv Rev 65:1357–1369
248. Li G, Huang Z, Zhang C, Dong BJ, Guo RH, Yue HW, Yan LT, Xing XH (2016) Construction of a linker library with widely controllable flexibility for fusion protein design. Appl Microbiol Biotechnol 100:215–225
249. Crivat G, Taraska JW (2012) Imaging proteins inside cells with fluorescent tags. Trends Biotechnol 30:8
250. Prescher JA, Bertozzi CR (2005) Chemistry in living systems. Nat Chem Biol 1(1):13–21
251. Ward WW, Prentice HJ, Roth AF, Cody CW, Reeves SC (1982) Spectral perturbations of the Aequorea green-fluorescent protein. Photochem Photobiol 35:803–808
252. Yang F, Moss LG, Phillips GN (1996) The molecular structure of green fluorescent protein. Nat Biotechnol 14(10):1246–1251
253. Swenson ES, Price JG, Brazelton T, Krause DS (2007) Limitations of green fluorescent protein as a cell lineage marker. Stem Cells 25:2593–2600
254. Wiedenmann J, Oswald F, Nienhaus GU (2009) Fluorescent proteins for live cell imaging: opportunities, limitations, and challenges. IUBMB Life 61:1029–1042
255. Ha T, Tinnefeld P (2012) Photophysics of fluorescent probes for single-molecule biophysics and super-resolution imaging. Annu Rev Phys Chem 63:595–617
256. Yang Z, Samanta S, Yan W, Yu B, Qu J (2021) Super-resolution microscopy for biological imaging. In: Optical imaging in human disease and biological research, pp 23–43

257. Schermelleh L, Ferrand A, Huser T, Eggeling C, Sauer M, Biehlmaier O, Drummen GPC (2019) Super-resolution microscopy demystified. Nat Cell Biol 21(1):72–84
258. Valli J, Garcia-Burgos A, Rooney LM, de Melo e Oliveira BV, Duncan RR, Rickman C (2021) Seeing beyond the limit: a guide to choosing the right super-resolution microscopy technique. J Biol Chem 297(1)
259. Lelek M, Gyparaki MT, Beliu G, Schueder F, Griffié J, Manley S, Jungmann R, Sauer M, Lakadamyali M, Zimmer C (2021) Single-molecule localization microscopy. Nat Rev Methods Prim 1(1):1–27
260. Dempsey GT, Vaughan JC, Chen KH, Bates M, Zhuang X (2011) Evaluation of fluorophores for optimal performance in localization-based super-resolution imaging. Nat Methods 8:1027–1040
261. Bates M, Huang B, Zhuang X (2008) Super-resolution microscopy by nanoscale localization of photo-switchable fluorescent probes. Curr Opin Chem Biol 12:505–514
262. Minoshima M, Kikuchi K (2017) Photostable and photoswitching fluorescent dyes for super-resolution imaging. J Biol Inorg Chem 22:639–652
263. Wang S, Moffitt JR, Dempsey GT, Xie XS, Zhuang X (2014) Characterization and development of photoactivatable fluorescent proteins for single-molecule-based superresolution imaging. Proc Natl Acad Sci U S A 111:8452–8457
264. Wu Z, Xu X, Xi P (2021) Stimulated emission depletion microscopy for biological imaging in four dimensions: a review. Microsc Res Tech 84:1947–1958
265. Sednev MV, Belov VN, Hell SW (2015) Fluorescent dyes with large Stokes shifts for super-resolution optical microscopy of biological objects: a review. Methods Appl Fluoresc 3(4): 042004
266. Jeong S, Widengren J, Lee JC (2022) Fluorescent probes for sted optical nanoscopy. Nanomaterials 12:21
267. Yang X, Yang Z, Wu Z, He Y, Shan C, Chai P, Ma C, Tian M, Teng J, Jin D, Yan W, Das P, Qu J, Xi P (2020) Mitochondrial dynamics quantitatively revealed by STED nanoscopy with an enhanced squaraine variant probe. Nat Commun 11(1):1–9
268. Lukinavičius G, Reymond L, D'Este E, Masharina A, Göttfert F, Ta H, Güther A, Fournier M, Rizzo S, Waldmann H, Blaukopf C, Sommer C, Gerlich DW, Arndt HD, Hell SW, Johnsson K (2014) Fluorogenic probes for live-cell imaging of the cytoskeleton. Nat Methods 11:731–733
269. Xu Y, Xu R, Wang Z, Zhou Y, Shen Q, Ji W, Dang D, Meng L, Tang BZ (2021) Recent advances in luminescent materials for super-resolution imaging via stimulated emission depletion nanoscopy. Chem Soc Rev 50:667–690
270. Sreedharan S, Gill MR, Garcia E, Saeed HK, Robinson D, Byrne A, Cadby A, Keyes TE, Smythe C, Pellett P, Bernardino De La Serna J, Thomas JA (2017) Multimodal super-resolution optical microscopy using a transition-metal-based probe provides unprecedented capabilities for imaging both nuclear chromatin and mitochondria. J Am Chem Soc 139: 15907–15913
271. Butkevich AN, Lukinavičius G, D'Este E, Hell SW (2017) Cell-permeant large Stokes shift dyes for transfection-free multicolor nanoscopy. J Am Chem Soc 139:12378–12381
272. Nienhaus K, Ulrich Nienhaus G (2014) Fluorescent proteins for live-cell imaging with super-resolution. Chem Soc Rev 43:1088–1106
273. Feld LG, Shynkarenko Y, Krieg F, Rainò G, Kovalenko MV (2021) Perovskite quantum dots for super-resolution optical microscopy: where strong photoluminescence blinking matters. Adv Opt Mater 9:2100620
274. Jin D, Xi P, Wang B, Zhang L, Enderlein J, Van Oijen AM (2018) Nanoparticles for super-resolution microscopy and single-molecule tracking. Nat Methods 15:415–423
275. Sharonov A, Hochstrasser RM (2006) Wide-field subdiffraction imaging by accumulated binding of diffusing probes. Proc Natl Acad Sci 103:18911–18916
276. Schwering M, Kiel A, Kurz A, Lymperopoulos K, Sprödefeld A, Krämer R, Herten DP (2011) Far-field nanoscopy with reversible chemical reactions. Angew Chem Int Ed 50:2940–2945

277. Gurskaya NG, Verkhusha VV, Shcheglov AS, Staroverov DB, Chepurnykh TV, Fradkov AF, Lukyanov S, Lukyanov KA (2006) Engineering of a monomeric green-to-red photoactivatable fluorescent protein induced by blue light. Nat Biotechnol 24:461–465
278. Ando R, Hama H, Yamamoto-Hino M, Mizuno H, Miyawaki A (2002) An optical marker based on the UV-induced green-to-red photoconversion of a fluorescent protein. Proc Natl Acad Sci U S A 99:12651–12656
279. Hoi H, Shaner NC, Davidson MW, Cairo CW, Wang J, Campbell RE (2010) A monomeric photoconvertible fluorescent protein for imaging of dynamic protein localization. J Mol Biol 401:776–791
280. Zhang M, Chang H, Zhang Y, Yu J, Wu L, Ji W, Chen J, Liu B, Lu J, Liu Y, Zhang J, Xu P, Xu T (2012) Rational design of true monomeric and bright photoactivatable fluorescent proteins. Nat Methods 9:727–729
281. Fuchs J, Böhme S, Oswald F, Hedde PN, Krause M, Wiedenmann J, Nienhaus GU (2010) A photoactivatable marker protein for pulse-chase imaging with superresolution. Nat Methods 7: 627–630
282. Adam V, Moeyaert B, David CC, Mizuno H, Lelimousin M, Dedecker P, Ando R, Miyawaki A, Michiels J, Engelborghs Y, Hofkens J (2011) Rational design of photoconvertible and biphotochromic fluorescent proteins for advanced microscopy applications. Chem Biol 18:1241–1251
283. Xia J, Kim SHH, Macmilllan S, Truant R (2006) Practical three color live cell imaging by widefield microscopy. Biol Proced Online 8:63–68
284. Subach OM, Patterson GH, Ting LM, Wang Y, Condeelis JS, Verkhusha VV (2011) A photoswitchable orange-to-far-red fluorescent protein, PSmOrange. Nat Methods 8:771–780
285. Chozinski TJ, Gagnon LA, Vaughan JC, Puchner EM, Huang B, Gaub HE, Just W (2014) Twinkle, twinkle little star: photoswitchable fluorophores for super-resolution imaging. FEBS Lett 588:3603–3612
286. Rust MJ, Bates M, Zhuang X (2006) Stochastic optical reconstruction microscopy (STORM) provides sub-diffraction-limit image resolution. Nat Methods 3:793
287. Bates M, Huang B, Dempsey GT, Zhuang X (2007) Multicolor super-resolution imaging with photo-switchable fluorescent probes. Science 317:1749
288. Tam J, Cordier GA, Borbely JS, Álvarez ÁS, Lakadamyali M (2014) Cross-talk-free multicolor storm imaging using a single fluorophore. PLoS One 9:e101772
289. Heilemann M, Margeat E, Kasper R, Sauer M, Tinnefeld P (2005) Carbocyanine dyes as efficient reversible single-molecule optical switch. J Am Chem Soc 127:3801–3806
290. Vaughan JC, Dempsey GT, Sun E, Zhuang X (2013) Phosphine quenching of cyanine dyes as a versatile tool for fluorescence microscopy. J Am Chem Soc 135:1197–1200
291. Vaughan JC, Jia S, Zhuang X (2012) Ultrabright photoactivatable fluorophores created by reductive caging. Nat Methods 9:1181–1184
292. Lehmann M, Gottschalk B, Puchkov D, Schmieder P, Schwagerus S, Hackenberger CPR, Haucke V, Schmoranzer J (2015) Multicolor caged dSTORM resolves the ultrastructure of synaptic vesicles in the brain. Angew Chem Int Ed 54:13230–13235
293. Goossen-Schmidt NC, Schnieder M, Hüve J, Klingauf J (2020) Switching behaviour of dSTORM dyes in glycerol-containing buffer. Sci Rep 10(1):1–8
294. Uno SN, Kamiya M, Yoshihara T, Sugawara K, Okabe K, Tarhan MC, Fujita H, Funatsu T, Okada Y, Tobita S, Urano Y (2014) A spontaneously blinking fluorophore based on intramolecular spirocyclization for live-cell super-resolution imaging. Nat Chem 6:681–689
295. Uno SN, Kamiya M, Morozumi A, Urano Y (2017) A green-light-emitting, spontaneously blinking fluorophore based on intramolecular spirocyclization for dual-colour super-resolution imaging. Chem Commun 54:102–105
296. Morozumi A, Kamiya M, Uno SN, Umezawa K, Kojima R, Yoshihara T, Tobita S, Urano Y (2020) Spontaneously blinking fluorophores based on nucleophilic addition/dissociation of intracellular glutathione for live-cell super-resolution imaging. J Am Chem Soc 142: 9625–9633

297. Thiel Z, Rivera-Fuentes P (2018) Photochemically active dyes for super-resolution microscopy. Chimia (Aarau) 72:764–770
298. Li B, Haris U, Aljowni M, Nakatsuka A, Patel SK, Lippert AR (2021) Tuning the photophysical properties of spirolactam rhodamine photoswitches. Isr J Chem 61:244–252
299. Fölling J, Belov V, Kunetsky R, Medda R, Schönle A, Egner A, Eggeling C, Bossi M, Hell SW (2007) Photochromic rhodamines provide nanoscopy with optical sectioning. Angew Chem Int Ed Engl 46:6266–6270
300. Bossi M, Föiling J, Belov VN, Boyarskiy VP, Medda R, Egner A, Eggeling C, Schönle A, Hell SW (2008) Multicolor far-field fluorescence nanoscopy through isolated detection of distinct molecular species. Nano Lett 8:2463–2468
301. Belov VN, Bossi ML, Fölling J, Boyarskiy VP, Hell SW (2009) Rhodamine spiroamides for multicolor single-molecule switching fluorescent nanoscopy. Chem – A Eur J 15:10762–10776
302. Uno K, Aktalay A, Bossi ML, Irie M, Belov VN, Hell SW (2021) Turn-on mode diarylethenes for bioconjugation and fluorescence microscopy of cellular structures. Proc Natl Acad Sci U S A 118:2100165118
303. Hauke S, Von Appen A, Quidwai T, Ries J, Wombacher R (2016) Specific protein labeling with caged fluorophores for dual-color imaging and super-resolution microscopy in living cells. Chem Sci 8:559–566
304. Jang S, Kim M, Shim SH (2020) Reductively caged, photoactivatable DNA-PAINT for high-throughput super-resolution microscopy. Angew Chem Int Ed 59:11758–11762
305. Klán P, Šolomek T, Bochet CG, Blanc A, Givens R, Rubina M, Popik V, Kostikov A, Wirz J (2013) Photoremovable protecting groups in chemistry and biology: reaction mechanisms and efficacy. Chem Rev 113:119–191
306. Banala S, Maurel D, Manley S, Johnsson K (2012) A caged, localizable rhodamine derivative for superresolution microscopy. ACS Chem Biol 7:289–293
307. Butkevich AN, Weber M, Cereceda Delgado AR, Ostersehlt LM, D'Este E, Hell SW (2021) Photoactivatable fluorescent dyes with hydrophilic caging groups and their use in multicolor nanoscopy. J Am Chem Soc 143:18388–18393
308. Betzig E, Patterson GH, Sougrat R, Lindwasser OW, Olenych S, Bonifacino JS, Davidson MW, Lippincott-Schwartz J, Hess HF (2006) Imaging intracellular fluorescent proteins at nanometer resolution. Science 313:1642–1645
309. Hess ST, Girirajan TPK, Mason MD (2006) Ultra-high resolution imaging by fluorescence photoactivation localization microscopy. Biophys J 91:4258–4272
310. Bates M, Blosser TR, Zhuang X (2005) Short-range spectroscopic ruler based on a single-molecule optical switch. Phys Rev Lett 94:108101
311. Shroff H, Galbraith CG, Galbraith JA, White H, Gillette J, Olenych S, Davidson MW, Betzig E (2007) Dual-color superresolution imaging of genetically expressed probes within individual adhesion complexes. Proc Natl Acad Sci 104:20308–20313
312. Li D, Shao L, Chen BC, Zhang X, Zhang M, Moses B, Milkie DE, Beach JR, Hammer JA, Pasham M, Kirchhausen T, Baird MA, Davidson MW, Xu P, Betzig E (2015) Extended-resolution structured illumination imaging of endocytic and cytoskeletal dynamics. Science 349(6251):aab3500
313. Hofmann M, Eggeling C, Jakobs S, Hell SW (2005) Breaking the diffraction barrier in fluorescence microscopy at low light intensities by using reversibly photoswitchable proteins. Proc Natl Acad Sci U S A 102:17565–17569